

Technical University of Crete

Department of Mineral Resources Engineering

Master of Science

Graduate Program in Geotechnology and the
Environment



Use of Spectral Induced Polarization in environmental applications

Konstantina Gerodimou

Chania 2017

Submitted to the School of Mineral Resources Engineering, Technical University of Crete

Supervising Committee:

Antonis Vafeidis, Professor, Technical University of Crete

Pantelis Soupios, Professor, TEI of Crete

Konstantinos Komnitsas, Professor, Technical University of Crete

Copying, storage and distribution of this work, in whole or part of it for commercial purposes is not allowed. Reproduction, storage and distribution for non-profit purposes, educational or research nature is permitted provided that the origin source is indicated and to maintain the existing message. Questions concerning the use of labor for profit should be addressed to the author.

The views and conclusions contained in this document reflect the author and should not be interpreted as reflecting official positions of Technical University of Crete.

Abstract

Geophysical prospecting in the past century has shifted its applicability from mineral exploration, as it was used in the beginning of the 20th century, to more environmental applications. Such applications included, but not limited, to environmental pollution, aquifer characterization, definition of pollutants at the subsurface. Probably the most applied methods are those based on the induction of electric current to the ground and measuring the voltage potential. Another method applied at the end of the century was the induced polarization, originally developed for the prospecting and characterization of mineral deposits. The value of the induced polarization (IP) method also has been recognized for near-surface studies in relatively low-polarizable, sedimentary environments. Nowadays it is used also for the characterization of hydraulic properties or the monitoring of biogeochemical processes in the subsurface.

An improvement of the IP method is the frequency-dependent complex electrical conductivity measurements, where the real part of the complex electrical conductivity is a measure of the ohmic conduction properties. The imaginary part represents polarization processes (Breede et al., 2012). The Spectral Induced Polarization (SIP) method allows for a more in-depth investigation of the electrochemical interactions between solutions and subsoil. The technique has also received important attention because of its potential application in hydrogeology (Slater2007).

This thesis presents the application of spectral induced polarization (SIP) method in a controlled laboratory experiment using biochar as remediation agent and textile waste water (TWW) as the contaminant. TWW industry is a creator of a huge amount wastewater and in many cases the disposal is uncontrolled. The TWW ends up in the aquifer and soil. The SIP method has proved to be an important qualitative monitoring tool for assessing the environmental quality in contaminated lands.

ACKNOWLEDGEMENTS

I would like to thank my supervisor Professor Vafeidis Antonis for his support from the begging of my master. He was very patient and supportive during the courses and he was always available for teaching me.

I am grateful to Professor Soupios Pantelis. Mr Soupios believed in my research but the most important thing was that he believed in me. He supported me in every step of my master and he was always available for guiding me in any difficulty I faced during the reaserch. I believe that from now on, he is not only my teacher but he is also a good friend.

Special thanks to professor Komnitsas Konstantinos who accepted to be part of my research.

I am particularly grateful to Professor Kalderis Dimitris for his willingness to support the chemical analysis of my research.

I am also grateful to professor Ntarlagiannis Dimitris for supporting the research. His advices were very significant for the experimental set up and his intervention in the SIP processing were more than important.

I want to thank Kirmizakis Panayiotis for his help in the beginning of the experiment.

I am very grateful in people who helped me with the interpretation of my research with their own way. Thank you Andrea Ustra for the Debye decomposition, Sina Saneiyan and Mr. Berkant Kayan.

I would like to thank the company TSAL S.A. (Pantelis Tsalapatas) for constructing the acrylic tube columns for the experiment without cost.

In the end, thanks to my family for the support and especially to my son Giorgos. Thank you Giorgos for teaching me how to be a better person.

CONTENTS

ABSTRACT.....	3
ACKNOWLEDGEMENTS.....	4
CONTENTS.....	5
LIST OF FIGURES.....	7
LIST OF TABLES.....	9
1. INTRODUCTION.....	10
1.1 literature review.....	10
1.2 Purpose of the thesis.....	11
1.3 Structure of the thesis.....	11
2. Theory-Methodology.....	12
2.1 Introduction.....	12
2.2 Induced Polarization (IP).....	13
2.3 Spectral Induced Polarization (SIP).....	15
2.4 Complex Conductivity in frequency domain.....	16
2.5 Mechanisms.....	18
2.5.1 Electrochemical Polarization.....	18
2.5.2 Maxwell-Wagner Polarization.....	18
2.5.3 Electrical Double Layer (EDL).....	21
2.6 Contaminant-Textile Wastewater (TWW).....	21
2.7 Decontamination Agent-Biochar.....	23
2.8 Adsorption.....	25
3. Experimental Set Up.....	26

3.1 Instruments.....	26
3.2 Calibration measurements.....	29
4.Laboratory measurements.....	31
4.1 Column preparation.....	31
4.2Experimental set up.....	34
5. Chemical Analysis.....	36
5.1 Spectrophotometers' calibration.....	37
5.2 Adsorption results.....	39
5.3 Adsorption curves.....	41
6. Results.....	42
7. Interpretation.....	48
7.1 SIP interpretation.....	48
7.1.1Frequency dependent.....	52
7.2.2Comparison geophysics vs geochemical.....	54
8. Conclusions.....	57
Refrences.....	59
Appendix A.....	63

List of figures

Figure 2.1. Induced Polarization IP signal in time domain. According the diagram, the trend change in the electrode with time and when the current is shut down abruptly it decays exponentially with time until it reach zero value (Papazachos 1996).....	14
Figure 2.2 Polarization of the electrodes (GeoSci Developers, Creative Commons Attribution 4.0 International License).....	15
Figure 2.3. Membrane Polarization (GeoSci Developers, Creative Commons Attribution 4.0 International License).....	15
Figure 2.4 For electrodes in the soil, two for current (c) and two for potential. The arrangement of the electrodes is dipole-dipole (Slater 2014).....	17
Figure 2.5 The graph shows one of the current frequencies which it has the same frequency with voltage as time changes. The time change with the phase lag (ϕ) is measured(Slater2014).....	17
Figure 2.6 Electrical double layer, diffuse and Stern layer (Slater 2014).....	19
Figure 2.7 Tortuosity in a porous media. The yellow line shows the way followed by the fluid in the soil (Slater 2014)	19
Figure 2.8 Circuit model of the electrical response (Vinegar and Waxman, 1984).....	20
Figure 2.9 TWW with strong red color (China daily Reuters).....	22
Figure 2.10. The chemical molecule of RR120.....	22
Figure 2.11 Biochar (BC1) after 2mm sieve treatment.....	24
Figure 2.12 Adsorption mechanism (Junior Golden. Heterogeneous catalysis, lecture 9).....	25
Figure 2.13 Physical vs chemical adsorption (Bartiomiej Gawel 2016).....	26
Figure 3.1. Portable SIP field/lab unit.....	27
Figure 3.2. Schematic of the column used (Kirmizakis 2016).....	27
Figure 3.3. The experimental chambers and the current/potential electrodes used are shown. Moreover, the valves at the bottom and on the top of the chamber for inflow and outflow of the contaminant used are also presented.....	28
Figure 3.4 Silver- silver chloride electrodes (Ag/Ag-Cl).....	28
Figure 3.5 Calibration measurements with KCL standard solution.....	30
Figure 3.6 Calculation of geometric factor for one of the used columns, lines for all electrode combinations.....	31
Figure 4.1 Columns with 10% biochar concentration.	33
Figure 4.2 Data acquisition using two different potential electrodes combinations (duplicate measurements).....	34
Figure4.3 Liquid filling.....	34

Figure 4.4 The collected raw data and a preliminary processing step are shown.....	36
Figure 5.1 Sample vial from the experimental outflow.....	36
Figure 5.2. UV mini 1240, UV-VIS spectrophotometer.SHIMADZU.....	37
Figure 5.3 Calibration curve for the RR120 aqueous solution. (Columns C1-C5)	38
Figure 5.4 Calibration curve for the RR120 aqueous solution. (Columns C6-C7).....	39
Figure 5.5 Column 1(reference) - column 5(10% biochar).....	41
Figure 5.6 Column 6- column 7 (20% biochar).....	41
Figure 5.7 Column 2 (100% biochar).....	42
Figure 6.1 Phase, imaginary and real conductivity for column 1 and P1-P5 electrode combination.....	43
Figure 6.2 Phase, imaginary and real conductivity for column 5 and P1-P5 electrode combination.....	44
Figure 6.3 Phase, imaginary and real conductivity for column 6 and P1-P5 electrode combination.....	45
Figure 6.4 Phase, imaginary and real conductivity for column 7 and P2-P4 electrode combination.....	46
Figure 6.5 Phase, imaginary and real conductivity for column 7(100%biochar and dionised water) and P2-P4 electrode combination. For the experiment with dionised water we had 12 loops.....	47
Figure 6.6 Phase, imaginary and real conductivity for column 7(100%biochar and RR120) and P2-P4 electrode combination. For the experiment with RR120, we had 15 loops.....	48
Figure 7.1. Temporal evolution for column 20% biochar+RR120. Peak frequency shifts towards higher frequencies. Average peak frequency 0.7Hz.The phase follows the degradation procedure.	49
Figure 7.2. Comparison shows that there is a phase change in the RR120 diagram and no change in the water diagram. It is a very clear result that the SIP method gives signal. The degradation process can detect.....	50
Figure 7.3. Column 100% biochar (RR & Water)-imaginary & real conductivity, phase and resistivity change at 1Hz.Clearly different phase magnitude and distinctively different trends.....	51
Figure 7.4 10% Biochar, Phase, Imaginary & Real conductivity, Resistivity change at PF: 63Hz.....	53
Figure 7.5 Frequency in 1000Hz.....	53
Figure 7.10 Integration of geophysical measurements with geochemical analysis. In the ellipse it has spotted the time that we observed the maximum change of the phase.....	54

Figure 7.11 Temporal evolution of the phase magnitude. The phase shift follows contaminant concentration decrease. Semi static. (10Hz).....55

Figure 7.12 Temporal evolution of the phase magnitude. The phase shift follows contaminant concentration decrease. Dynamic mode. (1Hz).....55

Figure 7.13 Temporal evolution of phase magnitude for 100% biochar (content). Dynamic mode in peak frequency 1Hz.....56

Figure 7.14 Visually evident. TWW before and after treatment.....57

List of Tables

Table 2.1 BC1 carbon used for our experiment and was fully characterized by Bachmann et al., (2016)(<http://pubs.acs.org/doi/abs/10.1021/acs.jafc.5b05055>).....24

Table 3.1. Composition of standard solutions according to ASTM D1125-95 method.....29

Table 3.2 Aqueous KCL Standard solutions- concentration.....29

Table 4.1 Mixture by volume.....32

Table 5.1 Absorbance results for RR120 ($\lambda=535\text{nm}$) Columns C1-C537

Table 5.2 Absorbance results for RR120 ($\lambda=535\text{nm}$) (Columns C6-C7).....38

Tables 5.3 Results of the absorption for all the columns used.....39

Table 8.1 Contaminant removals in (%); is depended from biochar's amount in the champers.....57

1. Introduction

1.1 Literature review

In recent years the scientific community studies and tries to solve important contamination problems as uncontrolled deposition of wastewater in the subsurface, surface water and aquifer. Lots of techniques have been tested with dominant electric methods.

Electromagnetic methods (radar) have also been used with significant results but for near surface applications. Electrical methods can be classified in invasive and non-invasive methods or passive methods and active methods. Passive methods are those that use naturally electric fields on earth and active methods are those that caused by injection of electrical current in to the earth using electrodes. A passive technique is the Self Potential (SP) method. One of the most important uses of the method according Parasnis (1986) is in mineral exploration. Active electric methods include ERI (Electrical Resistivity Imaging), IP (Induced Polarization) and SIP (Spectral Induced Polarization). ERI it's been the most popular electrical technique and it is caused by the injection of the electrical current and measuring the potential. The image is in 2D, 3D and sometimes to 4D and this is the reason that makes the method important. ERI has been used in salt water intrusion (Nguyen et al. 2009), characterization and monitoring of contaminant (Ntarlagiannis et al. 2016), mapping buried wastes (Tsourlos et al.2014).

Over the past two decades IP (induced polarization) an electric method has been used for contamination surveys. The extension of IP is the Spectral Induced polarization an application that arose in biogeophysics for monitoring and characterizing surface and subsurface biogeochemical conditions (Atekwana and Slater 2009). SIP is a method, which is used for hydro geological and environmental investigations (Revil et al 2012a). According a SIP overview by Kemna et al. (2012) who studied and correlated hydrological and biogeochemical properties with the spectral response, the authors suggested that SIP is a strong tool for characterization and monitoring in subsurface characteristics (pore and grain size, permeability, fluid chemistry, mineral precipitation, etc) at different environmental applications.

They have been several applications in laboratory scale and in the field. SIP measurements in clayey soils, simple sand, sand clay mixtures. Ustra et al. (2012), used a SIP laboratory experiment to investigate the sensitivity of the method to toluene contamination in clayey soils and concluded that their results from the SIP signature are not satisfactorily for using the method for monitoring toluene contamination to clayey soils. Another approach for SIP measurements on saturated sand-clay mixtures says that a SIP property of polarization in saturated porous media has significant response (Breede et al. 2010). In another approach complex conductivity measurement in low frequency in peat samples shows those peats

produce a phase peak. In this survey they were able to correlate physical and chemical properties of several peat samples (Ponziani et al.2011)

Very interesting conclusions came up from another study, laboratory survey for investigate the influence of pore fluid chemistry on complex conductivity and SIP response of BEREASANDSTONE (Lesmes et al 2001). In their approach, "SIP parameters are related to the physiochemical parameters that control the surface conductivity response of rocks and soils".

1.2 Purpose of the thesis

The purpose of the present survey is to exploit physicochemical changes between a contaminant and biochar in a closed chamber to get a Spectral induced polarization signal to create potential for geophysical monitoring tool.

1.3 Structure of the thesis

Chapter 2: The second chapter describes the theory of the spectral induced polarization and the mechanisms which apart the geophysical method. It also describes the contaminant we use, the decontamination agent and the main chemical reaction taken place during the experiment.

Chapter 3: The third chapter contains the experimental set up including the instrumentation.

Chapter 4: The fourth chapter describes the experiment, the preparation of the chambers, the saturation of the columns and the way we worked during the measurements.

Chapter 5: The fifth chapter refers to the chemical measurements and their results. We present the adsorption tables and curves which export the chemical's procedure.

Chapter 6: The sixth chapter contains the most representative results from the geophysical measurements. It contains the main diagrams from processing of the raw data.

Chapter 7: The seventh chapter refers to the interpretation of our results. Geophysical and Geochemical results put together and describe how chemical methods complement geophysics and the reverse.

Chapter 8: In the eighth chapter I summarize the conclusions of my research.

2. Theory-Methodology

2.1 Introduction

Environmental and Near Surface Geophysics

According Reynolds Geophysics is “The application of geophysical methods to the investigation of near surface biophysicochemical phenomena that are likely to have implications for the local environment.” Solid earth geophysics studies the interior of the earth (up to core) and near surface geophysics is concerned with upper crust.

Geophysical prospecting in the past century has shifted its applicability from mineral exploration, as it was used in the beginning of the 20th century to more environmental applications. Such applications are used to environmental pollution, aquifer characterization and definition of pollution at the subsurface, contaminant mapping and monitoring, Geohazards, geologic mapping and archaeology. The most applied methods are those based on the induction of electric current to the ground and measuring the voltage potential.

Environmental sciences are well developed in our country. Particularly, geophysical surveys performed on the soil surface (Lanz et al.1998, Benson et al. 1984) with purpose the long term monitoring of soil’s characteristic changes. Geophysical techniques are non-invasive or minimally invasive; provide accurate results because of their high spatial and temporal resolution and relatively low cost. They can also have been used by remote monitoring and operation to study soil properties applicable to geology, environments chemistry, environment engineering and geochemistry. The most commonly suggested methods for detection of pollutants in the subsoil are the electrical research methods as IP,SIP, ERI, SP(Cartwright and McComas 1968; Warner 1969; Stoller and Roux 1973; Klefstad 1975; Barker 1990; Ross et al.1990; Carpenter et al. 1990; Naudet et al. 2003,2004),due to their sensitivity in conductivity contrast (Meju 2000b;Tsourlos et al.2014).

At the end of the century a non-invasive electrical method called Induced Polarization in time domain was applied for the characterization of mineral deposits. Nowadays it is also used for the characterization of hydraulic properties of the monitoring of biogeochemical processes in the subsurface.

It has been observed that there is illegal wastewater deposition in land fields and aquifer.. Geophysical methods can be used in such cases to find out the pollution boundaries, and characterize the soils properties receiving the load. For more accurate results for the type of the pollution, borehole sampling can be used. They procure continuous profiles and point measurements and give tomographic images. They can be applied in single boreholes, cross-borehole and multi-borehole configuration (Rubin and Hubbard 2005a; Reynolds 2011).

The electrochemical interaction between electrolyte and the mineral surface in the presence of the waste has grown interest (Sauck et al. 1998; Abdel et al. 2004; Kemna et al. 2004), due the electrical resistivity's property to be very sensitive to chemical composition of fluids, the soil's porosity and the degree of saturation (Waxman and Smits 1968). The Induced Polarization method is used to operate physiochemical characteristics in environmental monitoring. Also dielectric permittivity (ϵ_r) has recently been studied because of its relationship with imaginary conductivity due to the possibility to express electrical properties of the soil (Prodan et al. 2004). Joyce (2007) suggested that the SIP method is sensitive to environmental contaminants (nanomaterials, hydrocarbon) in natural systems, but also to the physiochemical changes in the sediments resulting from contamination.

Surveys mentioned above suggest that the SIP technique, an extension method of IP whose theory is described in the following pages, is proper to monitor environmental pollution in the subsurface.

The scientific community knowing the advantages of geophysics (fast results, financial interest, and high spatial and temporal resolution) decided the development of Biogeophysics improving the methods already existing for monitoring environmental pollution.

Biogeophysics enables correlation between geochemical analyses and parameters calculated from the geophysical methods. Biogeophysical methods record changes in geophysical parameters and they are interpreted as geochemical and biological environment changes that happen at the subsurface due to the presents of waste.

Biogeophysical methods were introduced by Rutgers University and Oklahoma State university researchers (Williams et al. 2005; Ntarlagiannis 2007; Persona et al. 2008; Ntarlagiannis and Ferguson 2009; Atekwana and Slater, 2009; , Slater 2006, 2007a, b, 2009;).

2.2 Induced Polarization (IP)

To understand the Spectral Induced Polarization (SIP) method it is necessary to explain the IP mechanisms. SIP is the extension of Induced polarization and the main difference between them is that in SIP we measure in the frequency domain.

Electrical methods apply electrical current through the subsurface using two electrodes for current injection and two electrodes for measure voltage potential. Once it is shut off abruptly, the voltage does not reach zero value at once. It decays exponentially with time and takes several seconds until it reaches zero. This is due to the property of the soil to act as a capacitor and store electric charge. Induced polarization is taking place due the electrochemical reactions. It can be produced between mineral grains in the soil or voltage

potential between contact surfaces of rocks with electrolytes. Using the IP method, we can measure polarization and chargeability (Papazachos 1986).

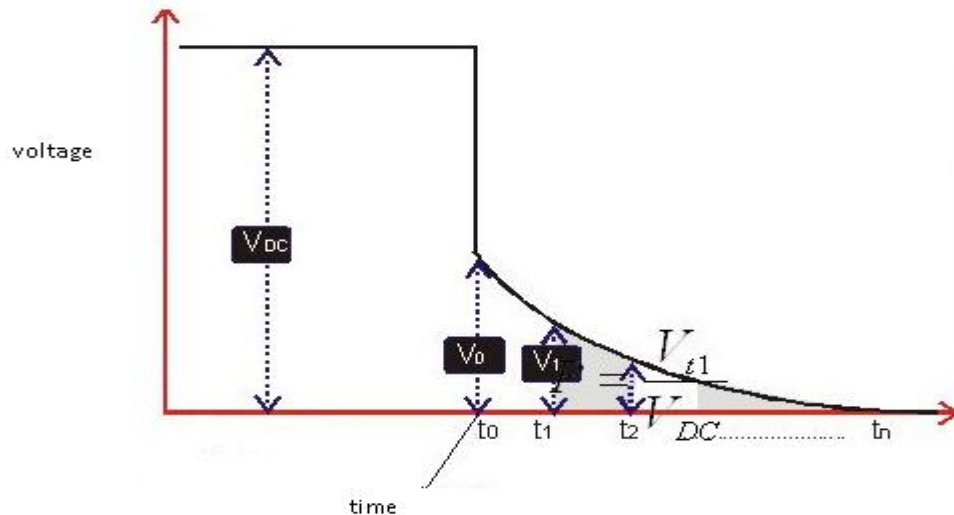


Figure 2.1 Induced Polarization IP signal in time domain. According to the diagram, the trend change in the electrode with time and when the current is shut down abruptly it decays exponentially with time until it reaches zero value (Papazachos 1996).

The phenomenon of the induced polarization caused by electrochemical reactions in the soil and two different reactions appear as the mechanism is working. The first is the polarization of the electrodes, caused by metallic granules present in porous rocks. When we inject current in the soil the granules are encircled by positive and negative ions and in the sides of the minerals counter ions appear. When we stop the current injection the granule acts like an electrical source and the current decays exponentially with the time.

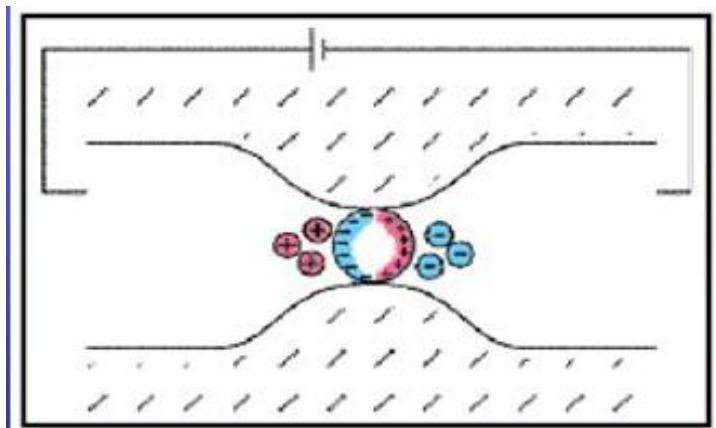


Figure 2.2 Polarization of the electrodes (GeoSci Developers, Creative Commons Attribution 4.0 International License).

The second source is the membrane polarization without geophysical interest and it acts like noise.

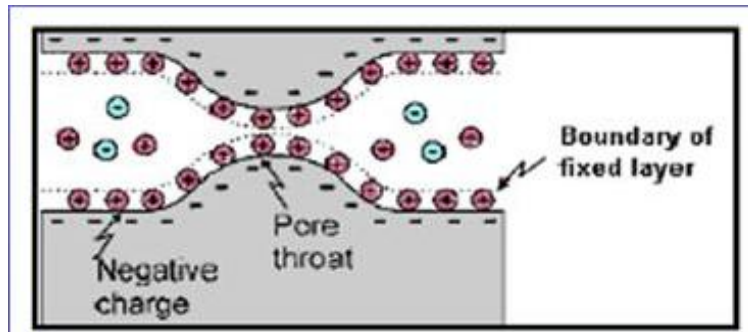


Figure 2.3 Membrane Polarization (GeoSci Developers, Creative Commons Attribution 4.0 International License).

2.3 Spectral Induced Polarization (SIP)

The SIP method has been used in recent years for contaminant monitoring and remediation. The method has been shown that it is sensitive to the physiochemical changes as a result of the contamination in a porous material. Spectral induced polarization (SIP) is initiated as the traditional IP method but the measurements are represented by a complex conductivity in a range of frequencies. There are a few mechanisms, which are taking place during the measurements as electrochemical polarization such as the Maxwell-Wagner polarization and the electrical Double Layer. The mechanisms are depended on the frequency magnitude and the nature of the material involved.

Complex conductivity is given by,

$$\sigma(\omega) = \frac{1}{\rho(\omega)} = \sigma'(\omega) + i\sigma''(\omega) \quad (2.1)$$

Where

$\rho(\omega)$: complex resistivity

ω :angular frequency

$$i = \sqrt{-1} \quad (2.2)$$

In the complex conductivity method we measure the magnitude,

$$|\sigma| = \frac{1}{|\rho|} = \sqrt{(\sigma')^2 + (\sigma'')^2} \quad (2.3)$$

And the phase angle,

$$\phi \quad (2.4)$$

In a range of frequencies and after following the equations above, we can calculate the real and the imaginary conductivity. The real conductivity (σ') represents ohmic conduction which is the energy loss and the imaginary conductivity (σ'') represents polarization which is the energy storage, to guide current in the soil.

In addition, real conductivity represents the reaction between the fluid chemistry and surface conductivity. Imaginary conductivity is electrical polarization between the interface and porous between the grains.

The phase shift concerns the reaction between the sediment and the current.

2.4 Complex resistivity in frequency domain

In the graphs above, we presented the method by physical view. We explained what happens during the current injection in field measurements. The method works exactly the same way even in controlled laboratory work.

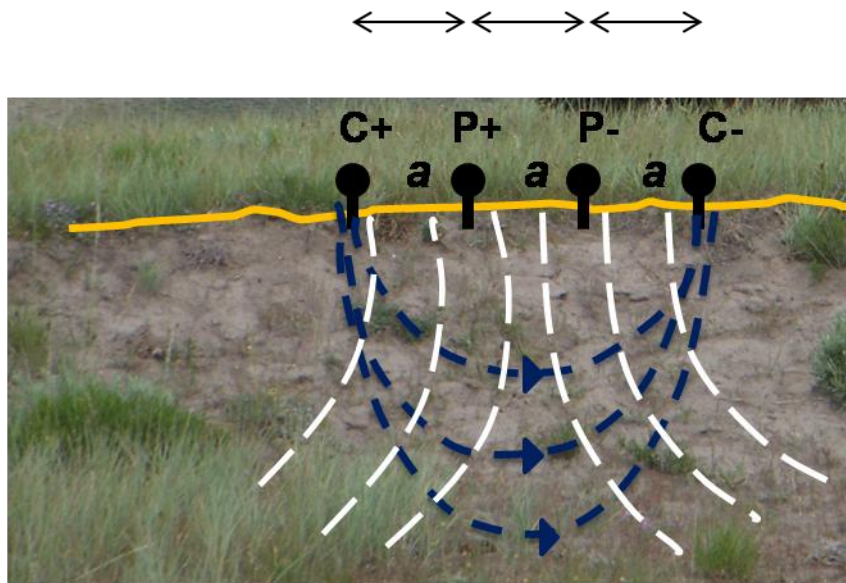


Figure 2.4 Four electrodes in the soil, two for current (c) and two for potential. The arrangement of the electrodes is dipole-dipole (Slater 2014).

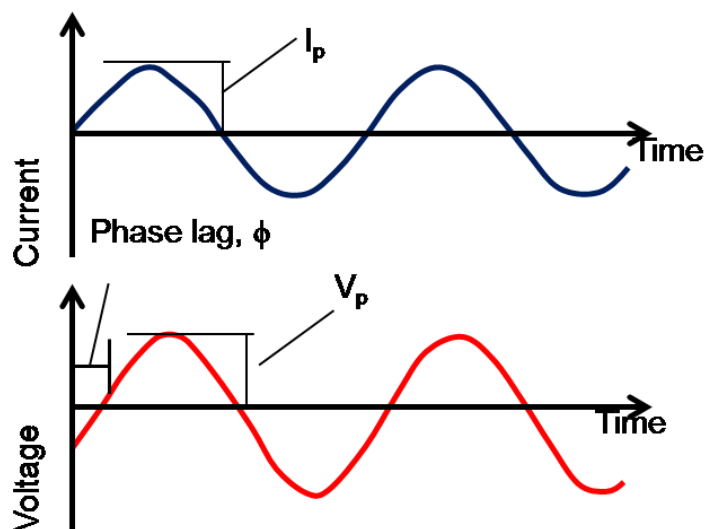


Figure 2.5 The graph shows one of the current frequencies which it has the same frequency with voltage as time changes. The time change with the phase lag (ϕ) is measured (Slater2014).

2.5 Mechanisms

During the SIP measurements a few mechanisms take place as :(i) electrochemical polarization and (ii) Maxwell-Wagner (MW) polarization (Leroy et al.2008, Leroy and Revil 2009) and (iii) electrical double layer (EDL) which is the main mechanism for the measurement in this thesis.

2.5.1 Electrochemical Polarization

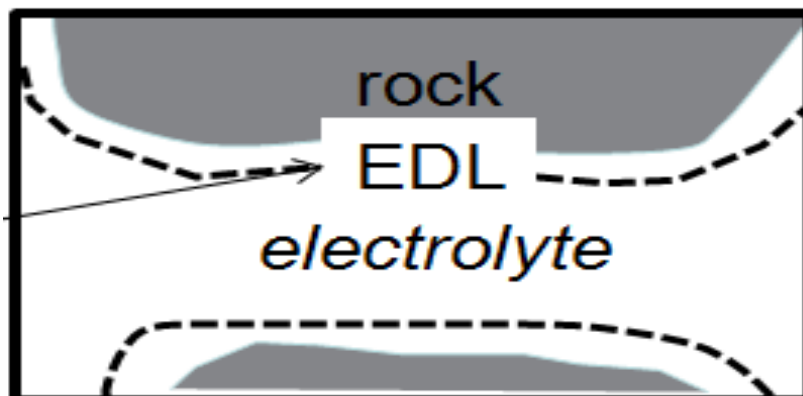
Electrochemical polarization arises from the polarization of the ions in the electrical double or triple layer at the grain-electrolyte interface.

2.5.2 MW polarization

Maxwell-Wagner (MW) polarization appears at the interfaces and discontinuities between the faces of a composite medium as the charges pile up during the change of the electric field. Most of the time the electrochemical polarization prevails at lower frequencies and MW can prevail at higher frequencies. The phases in the porous composite are different and they have different conductivities and different permittivity's (Leroy et al 2008; Leroy and Revil 2009).

2.5.3 EDL

The double layer is a structure that appears when the rock is exposed to the electrolyte. There are two parts of the electrical double layer, the inner part, which is the Stern layer, and the outer part which is the diffuse layer.



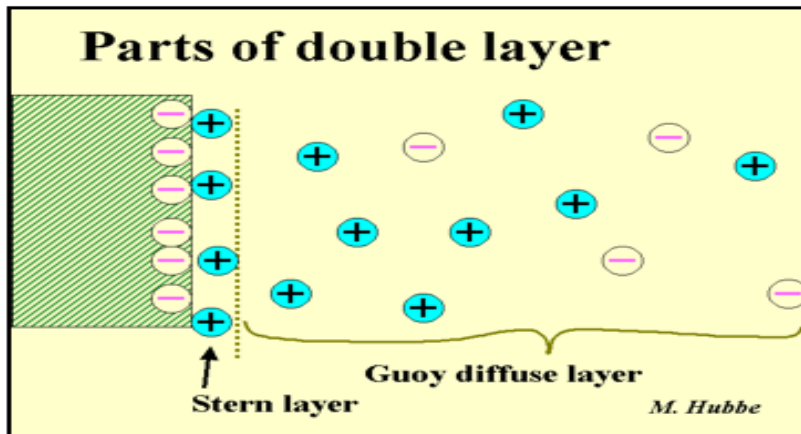


Figure 2.6 Electrical double layer, diffuse and Stern layer (Slater 2014).

The electrical double layer is controlled by Tortuosity. Tortuosity is defined as the fluid diffusion in a porous media. While a fluid diffuses in soil, it follows the easier path to fill the porous media. The fluid moves between the rocks and creates the EDL while it comes in contact with the rocks.

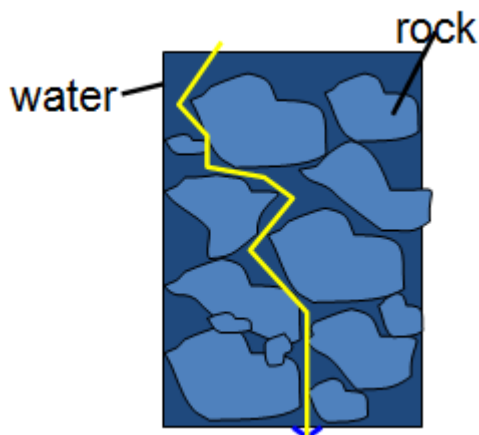


Figure 2.7 Tortuosity in a porous media. The yellow shows the way followed by the fluid in the soil (Slater 2014)

When the EDL is polarized, a frequency dependent complex surface conductivity appears. In the EDL, the migration and the polarization of the ions are checked by the frequency response of the complex conductivity. When you add in parallel the bulk electrical properties of the sample you use with the complex surface conductivity, the response of the sample you get is,

$$\sigma^* = (\sigma_{\text{bulk}} + i\omega\kappa\infty\epsilon_0) + [\sigma'_{\text{surf}}(\omega) + i\sigma''_{\text{surf}}(\omega)] \quad (2.5)$$

When

σ_{bulk} = the low frequency conductivity and

κ_{∞} = high frequency dielectric constant

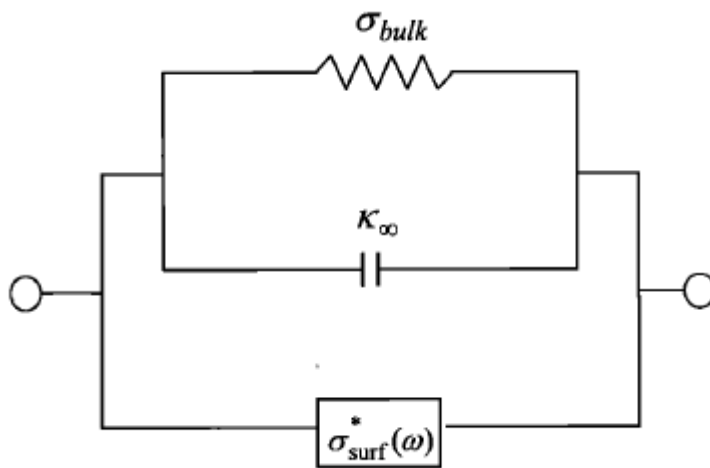


Figure 2.8 Circuit model of the electrical response (Vinegar and Waxman, 1984).

The bulk granules properties σ_{bulk} and κ_{∞} are independent from the frequency and they refer to the bulk grain sample. They are also given by the Hanai-Bruggeman theory (Sen et al 1981) which describes the low frequency conductivity response given by the Archie's law (Archie 1942)

$$\sigma_{\text{bulk}} = \sigma_w \varphi^m \quad (2.6)$$

where,

σ_w = solution conductivity

φ = porosity

m = cementation index (grain shape)

2.6 Contaminant Used - Textile Wastewater

Inorganic contaminants are compounds found in water and most of them are manmade through industry and agriculture or are natural made by the environment. These compounds are dangerous for the public health when they deposited without processing in the environment. We chose textile wastewaters (TWW) pollutants because they are broadly produced by textile industries. SIP method has been used as detection method of inorganic contaminants. The textile industry produced huge amount of wastewater. The textile wastewaters (TWW) are aqueous solutions with processed industry dyes. According researches (Paul et. al 2012), these effluents contain chemicals (acids, dyes, alkalis) which cause serious environmental pollution. The main characteristics of textile wastewater are strong color (red, brown, blue, purple black) and at the industry process during the day it is possible to change many times the color. The TWW color is the main negative impact for aquifer because of the absorption and reflection of sunlight in the water. If the TWW relished into the environment without processing, mainly by removing the dyes it has a huge impact at the photosynthetic activity. Dyes have the ability to remain in the environment for a big period because they are photo stable compounds. Another reason why textile wastewater requires treatment it is the degradation of the water quality related to acute and chronic effects.

This type of effluents can be treated by advanced processes (Fenton, photocatalisys), physicochemical methods (filtration, adsorption, and ion exchange), chemical methods (like ozonation, permanganate) and biological methods (aerobic and anaerobic decomposition).

Another characteristic of TWW with strong negative point is pH, caused by the variety of dyestuff, pH fluctuates between 2 and 12(Gurnham, 1965). The variation of dyestuff also causes fluctuation of COD and BOD.

According (Lin and Lin 1992) TWW are categorized in 3 types of COD: 1.high strength 1600 mg/lit 2.medium strength between 1600mg/lit-800mg/lit and 3.low strength lower than 800mg/lit.



Figure 2.9 TWW with strong red color (China daily Reuters).

2.6.1 Reactive Red 120

In this thesis we chose to use the dye Reactive Red 120 (RR120) because it was the most well defined dye widely used in other similar experiments. The linear formula of the dye is ($C_{44}H_{24}C_{12}N_{14}Na_6O_2S_6$) and the molecular weight 1469.34 g/mol. This dye is easy to apply in cellulosic fibers, wool and nylon.

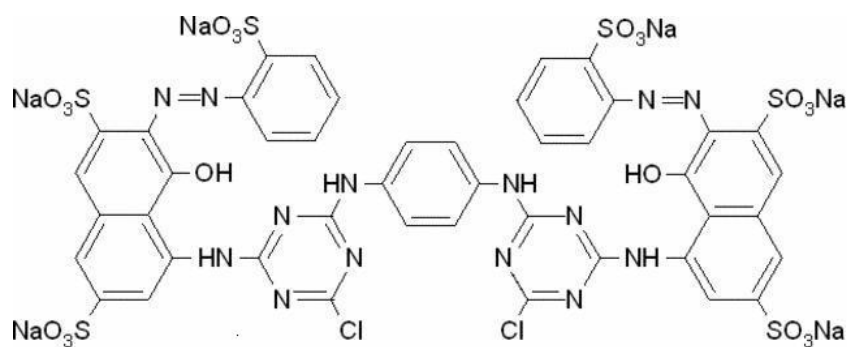


Figure 2.10 The chemical molecule of RR120

<https://www.google.gr/url?sa=t&rct=j&q=&esrc=s&source=web&cd=1&cad=rja&uact=8&ved=0ahUKEwqiqv7uogYjQAhWEPZoKHfR5CgYQFgghMAA&url=http%3A%2F%2Fwww.sigmaaldrich.com%2Fcatalog%2Fproduct%2Fsigma%2Fr0378&usg=AFQjCNG6pY6RGJyleCWBlrvXXLYGiF1wBg>

Reactive is a dye that operates with structure and reacts chemically with the substrate. Rattee and Stepheness (1954) have discovered the reactives at the Imperial Chemical Industry (ICI) in UK in 1954.

The efficient method for mineralization and decolourization of RR120 is the WAO (wet air oxidation) process that contains ozonation, photocatalysis and adsorption with natural material. It also contains gamma radiation and electrochemical degradation.

2.7 Decontamination agent - Biochar

The purpose of the experiment from physicochemical view is the discoloration of the effluent through the adsorption with biochar. Biochar is a solid heterogeneous substance produced by biomass pyrolysis. The IBI (International Biochar Initiative) term is "biochar is a solid material obtained from the carbonization of biomass". It has lots of uses such as tillage, building materials, water remediation, as a plant nutrition and in textile industry due its physicochemical properties. Biochar has several applications in organics remediation, phenols removal (Karakoyun et al. 2011; Kasozi et al. 2010), pesticides and polynuclear aromatics removal (Klasson et al 2013; Chen and Chen 2009), solvents removal (Chun et al 2004) and color/dye removal that is the issue of this work.

As mentioned above, biochar produced through pyrolysis process. Pyrolysis is the thermal decay of biomass in the absence of oxygen and it depends on operating conditions such as temperature, heating time and vapor residence time. There are six types of Pyrolysis (1) slow Pyrolysis, heating temperature about 500 °C from 5 to 30 min, (2) fast Pyrolysis, heating temperature of biomass in a range of 850-1300 °C and vapor residence from 1 to 10 s, (3) flash Pyrolysis, very high temperature in a very short period of time, (4) vacuum Pyrolysis, procedure in low pressure and oxygen absence (5) intermediate Pyrolysis (6) Hydrolysis.

The IBI has proposed a classification for biochar based in carbon content. Class 1 biochar (60% carbon or more), Class 2 biochar (between 30-60% carbons) Class 3 biochar (between 10%-30% carbon).

The origin of the feedstock includes variety, but predominant materials are usually wood and straw. Biochar more common characteristics are, concentration of elemental constituents, density, porosity and hardness (Spokas et al. 2012). The blend of biomass was pyrolyzed with PYREG 500-III Pyrolysis units (PYREG GmbH, Dorth, Germany) by Swiss Biochar (Lausanne, Switzerland), Sonnenerde GmbH (Riedlingsdorf, Austria) and PYREG GmbH produce BC1, BC2, BC3. In this thesis, we used biochar (BC1) from wood chip production with slow pyrolysis (20 min at 620 °C).



Figure 2.11 Biochar (BC1) after 2mm sieve treatment.

The main ingredient is the organic carbon through which we can identify biochar's type. Below there is a table of the concentrations of the most important elemental constituents of (BC1). The organic matter varies from feedstock and pyrolysis conditions.

Biochar is chosen instead of active carbon for economy reasons, it has lower production cost, fewer production steps and in most cases exactly the same results as an adsorbent

Table 2.1 BC1 carbon used for our experiment was fully characterized by Bachmann et al., (2016)(<http://pubs.acs.org/doi/abs/10.1021/acs.jafc.5b05055>)

Group	Parameter	sample	unit	Mean value	Reference value	Number of Labs results	Reproducibility SD Absolute relative	Horwitz function Value ratio	Repeability SD Absolute relative
CHNOS & ash	C	BC1	%	81.9	81.2	14 35	5.2 6.4%	1.7 3.1	2.0 2.4%
	H	BC1	%	1.48	1.19	10	0.31 21.0%	0.06 5.5	0.12 8.2%
	N	BC1	%	0.35	0.42	13 36	0.21 59.3%	0.02 12.4	0.02 5.6%
	O	BC1	%	5.8	3.8	4 9	2.0 35.3%	0.2 11.5	0.2 2.9%
	S	BC1	%	0.042	-	4	0.067 160.6%	0.003 22.3	0.067 160.6%
	S_ICP_OES	BC1	%	0.02	0.02	5 10	0.02 112.2%	0.00 21.0	0.00 6.9%
	Ash	BC1	%	11.35	13.30	14 25	3.58 31.5%	0.31 11.7	1.04 9.5%
	Main elements	P	BC1	mg/kg	765	870	5 11	152 19.8%	45 3.4
	K	BC1	mg/kg	6'763	9'400	8 1	4'144 61.3%	287 14.4	111 1.6%
	Na	BC1	mg/kg	103	690	8 1	52 50.5%	8 6.3	8 7.8%
	Mg	BC1	mg/kg	1'724	2'320	8 19	489 28.4%	90 5.4	25 1.5%
	Mn	BC1	mg/kg	301	-	7 1	66 22.0%	20 3.2	5 1.5%
	Cu	BC1	mg/kg	21'705	33'700	8 19	14'083 64.9%	773 18.2	629 2.9%
	Fe	BC1	mg/kg	1'087	1'840	8 19	492 45.3%	61 8.1	38 3.5%

Further parameters	pH	BC1		9.91	8.3	19 44	0.56 5.7%	-	-	0.03 0.3%
	EC	BC1		1'203	989	13 33	826 68 .7 %	-	-	31 2.6%
	SSA	BC1		316.0	224.8	8 13	58.3 18.5%	-	-	0.4 0.1%

2.8 Adsorption

The experiment we chose to perform it includes a contaminant, the textile wastewater and a remediation agent, biochar. The geophysical method we used is Spectral Induced Polarization (SIP). The purpose was to examine if there is a SIP signal during the decontamination procedure and study the ability of SIP as a monitoring tool. The chemical procedure that took place into the experiment chamber was the adsorption.

Increase in the concentration of a substance at the interface of a condensed and a liquid or gaseous layer owing to the operation of surface forces called adsorption (IUPAC definition). Adsorption is the adhesion of atoms, ions or molecules from liquid to a surface. For the experiment described the surface is biochar (BC1) and it is sensitive to toxic pollutants. The binding forces between atoms, molecules and ions are stronger during the adsorption at surface or interface (Robert, 1989).

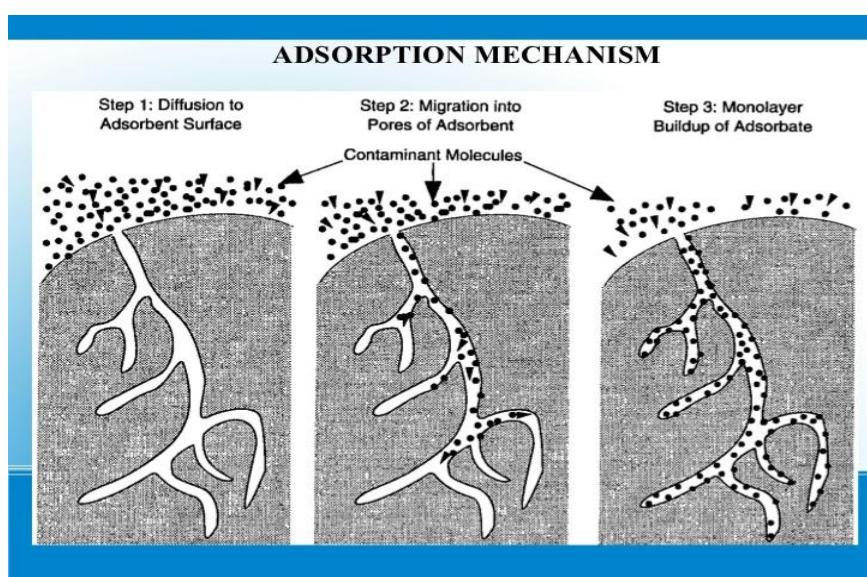


Figure 2.12 Adsorption mechanisms (Junior Golden. Heterogeneous catalysis, lecture 9)

There are two types of adsorption:

1. Physical adsorption: there is no electrons exchange between the solid and the fluid material and the adsorption is happening due the Van der Waals forces and hydrogen binding.
2. Chemical adsorption: it is about reaction of electrons between the adsorbed species and the adsorbent. The result of a chemical adsorption is bond stronger and more stable.

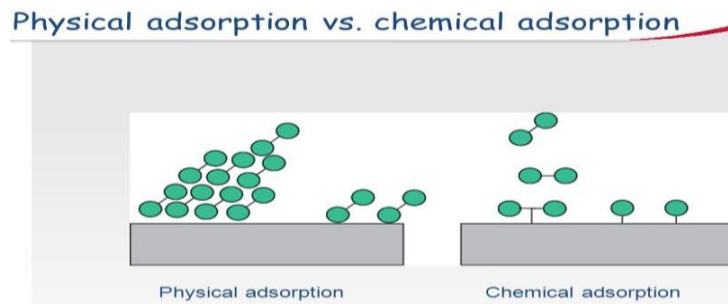


Figure 2.13 Physical vs chemical adsorption (Bartiomiej Gawel 2016)

Since we know the adsorptive capacity of biochar we used it as adsorbent in the experiment. During the adsorption in the chamber from the RR120 aqueous solution to biochar the purpose of the experiment is to record the SIP response associated with adsorption. During the geophysical measurements, we took samples of the fluid and at the same time in the laboratory of chemistry we measured the adsorption in the spectrophotometer.

3. Experimental Set Up

3.1 Instruments

The whole experiment was constructed from the beginning. A portable SIP field/lab unit with 2 current and 6 potential channels, by Ontash company

(<http://www.ontash.com/products.htm>) used for this research work.

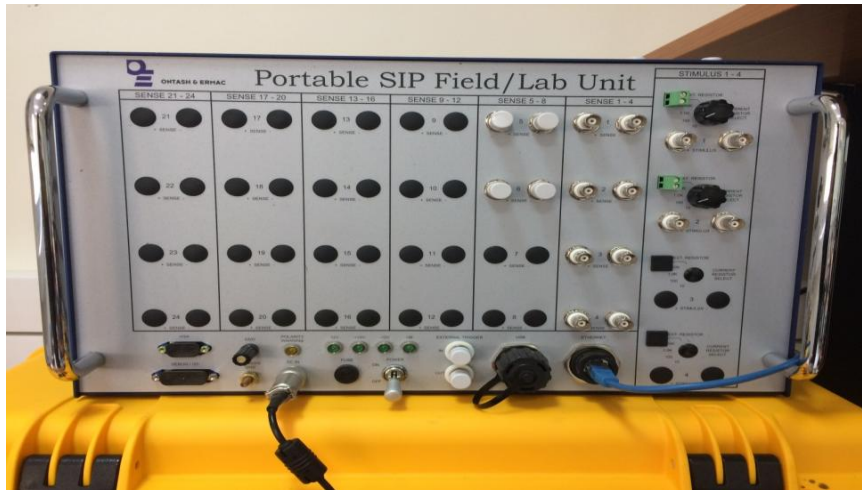


Figure 3.1 Portable SIP field/lab unit.

The instrument has the ability to measure the electric current at two injection channels at the same time and eight potential channels at different combinations.

The columns have three connecting valves from the one side for sampling or inject contaminant and five receptors to the other side for the potential electrodes. In the top and the bottom of the column, there are valves for the inflow fluid and the current potential electrodes.

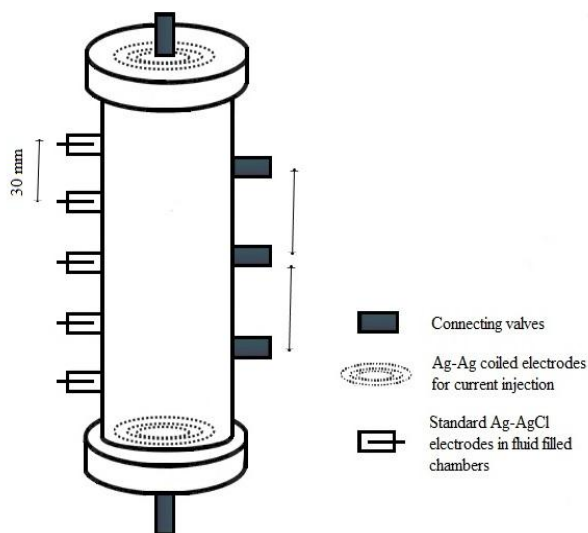


Figure 3.2 Schematic of the column used (Kirmizakis 2016).

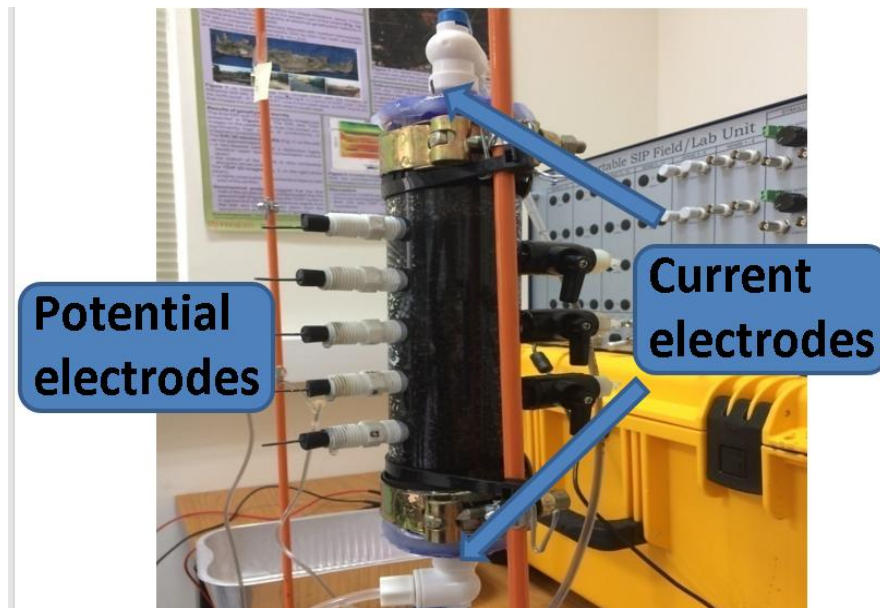


Figure 3.3 The experimental chamber and the current/potential electrodes used are shown. Moreover, the valves at the bottom and on the top of the chamber for inflow and outflow of the contaminant used are also presented.

The pure silver electrodes were turned in non-polarized (Ag/AgCl) with the method of immersion in chlorine. It was necessary to be nonpolarized to minimize potential electrode polarization (Vanhala and Soininen 1995; Ulrich and Slater 2004).



Figure 3.4 Silver- silver chloride electrodes (Ag/Ag-Cl)

3.2 Calibration measurements

Within the preparation of the experiment, calibration measurements were performed. The purpose was to calibrate the instrument with each column and to calculate the geometric factor. Columns during the calibration measurements were filled only with the standard solution.

For the calibration measurements, we used three aqueous KCL standard solutions with different concentrations. Each column was calibrated with the 3 standard solutions. The preparation of the solution was made in Chemistry's laboratory (TEI CRETE) according to the method ASTM D1125-95. We measured voltage potential in 4 different electrode combinations (P1-P2), (P3-P5), (P1-P4), (P1-P5) and the results are represented by the diagrams below. After the end of every set measurement, we have been collected a small amount of the solution to measure its conductivity.

Table 3.1 Composition of standard solutions according to ASTM D1125-95 method.

Conductivity	Molarity	Tolerance (at 25°C)
147 $\mu\text{S/cm}$	0.001 M	$\pm 5 \mu\text{S/cm}$
1413 $\mu\text{S/cm}$	0.01 M	$\pm 12 \mu\text{S/cm}$
12.88 mS/cm	0.1 M	$\pm 0.11 \text{ mS/cm}$

Table 3.2 Aqueous KCL Standard solutions- concentration

Conductivity	Molarity	Quantity of KCL (gr/L)
70 $\mu\text{S/cm}$	0.00047 M	0.035 gr/L KCl
300 $\mu\text{S/cm}$	0.002 M	0.14 gr/L KCl
900 $\mu\text{S/cm}$	0.0061 M	0.45 gr/L KCl

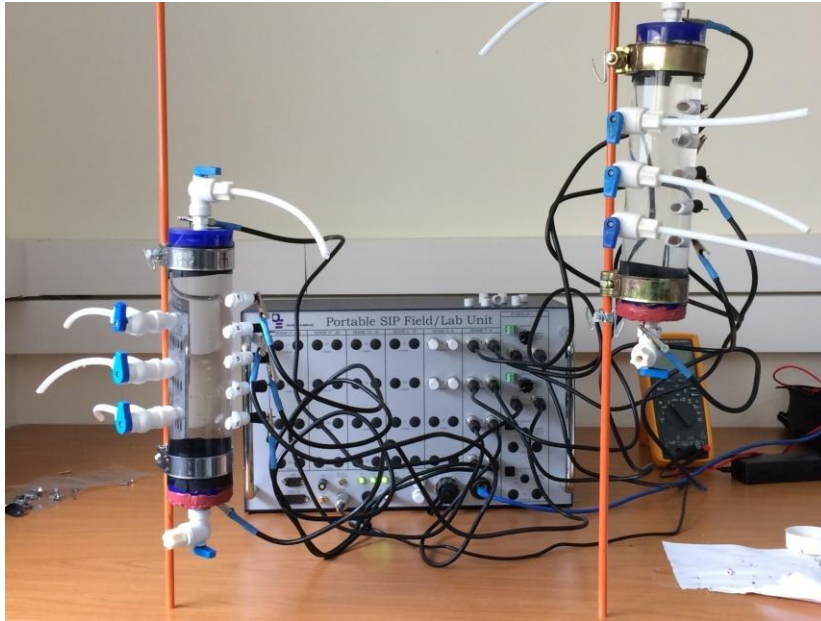


Figure 3.5 Calibration measurements with KCL standard solution.

The Geometric factor can be calculated by the graph of the fluid conductivity to conductance

$$Conductance = \frac{1}{Resistance} \cdot 1.000.000 \quad (3.1)$$

Moreover, by having the inverse of the slope and replacing it in the equation above we are in place to calculate the real fluid conductivity ($\mu\text{S}/\text{cm}$).

$$Fluid\ conductivity = \frac{1}{Resistance} \cdot K(\text{geometric factor}) \cdot 1.000.000 \quad (3.2)$$

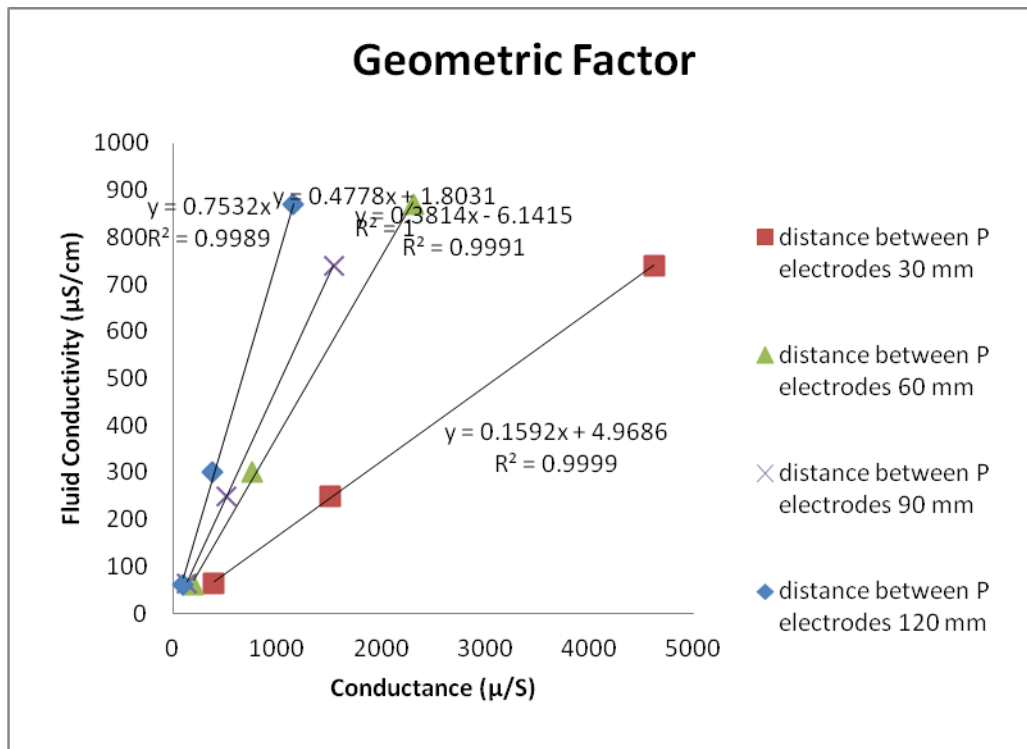


Figure 3.6 Calculation of geometric factor for one of the used columns, lines for all electrode combinations.

4. Laboratory measurements

4.1 Column preparation

For the experiment, we used biochar (BC1), Ottawa sand as buffer zone and aqueous solution RR120. Since we did not know the optimum mixture of biochar and sand for the best SIP signal, it was necessary to try different mixtures. Each column had its twin, except the reference column that was filled only with Ottawa sand. Ottawa sand it is standard sand,

clear, homogeneous and inert material. Meanwhile in chemistry laboratory we prepared the RR120 aqueous solution with concentration 100mg/lit and inflow conductivity 940 $\mu\text{S}/\text{cm}$.

The experiment was duplicate, not only because of the existence of the second identical column but also because every measurement set originated from two combinations of potential electrodes. Therefore, if for some reason data from one combination was lost there was raw data from the other one.

Table 4.1 Mixture by volume

	Content 100%	Content 10% (By volume (%))	Content 20% (By volume (%))
Biochar	100	10	20
Ottawa sand	0	90	80
Total Mixture	100	100	100

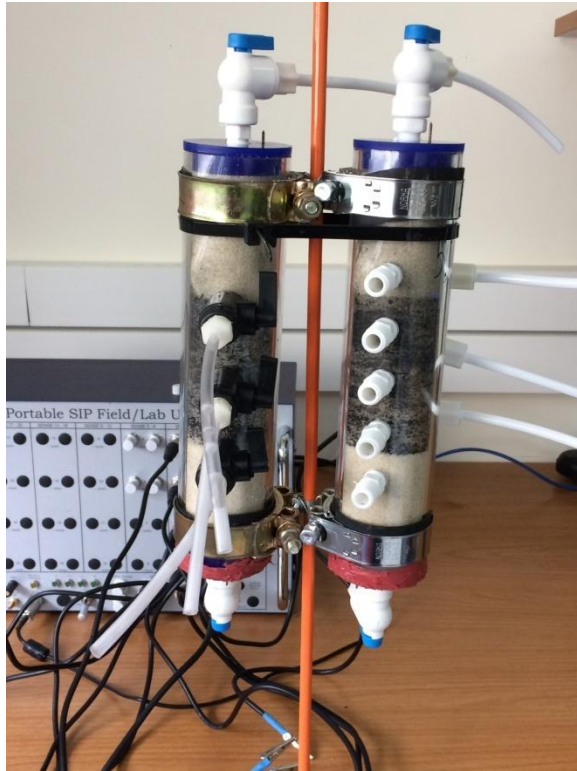


Figure 4.1 Columns with 10% biochar concentration.

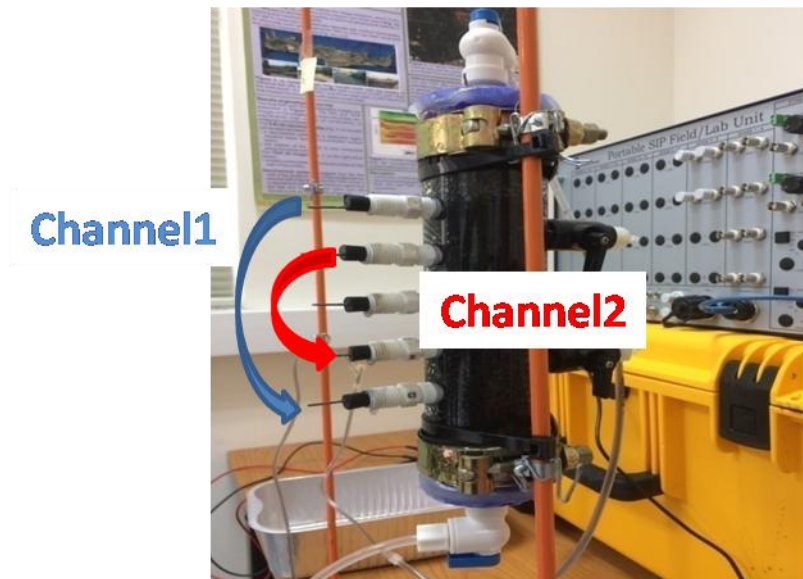


Figure 4.2 Data acquisition using two different potential electrodes combinations (duplicate measurements).



Figure 4.3 Liquid filling

4.2 Experimental set up.

Starting the experiment setup, we checked if the small filling pipes were clean and we started the flow to check first if there were any bubbles in the pipe. Bubbles in the chambers MAY block the SIP signal. After the in situ measurement of the inflow conductivity, the columns were fully saturated with the contaminant fluid.

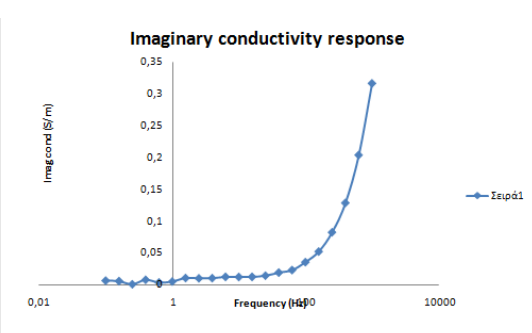
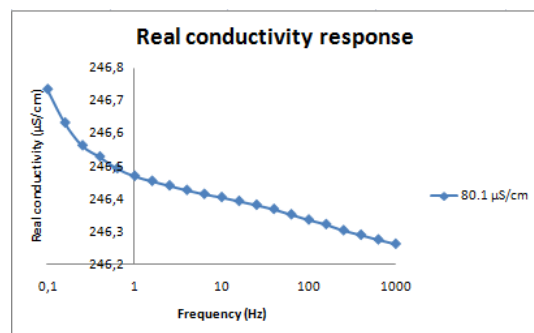
The filling flow was very slow to avoid channeling in the chamber as the fluid was going in the top of the column. Any dissimilarity between the grains it may disturb the system's balance. The last step before turning the instrument on and starting the measurements was to check with the conductivity meter and the voltage potential electrodes to ensure closed circuit in all combinations. The electrode combinations we used for the main experiment was (P1-P5) and (P2-P4), the distance between the electrodes was 0.06m and 0.12m respectively. The electrode P3 was left as a spare.

We separate the experiment process in two parts namely dynamic and semi-static mode. We decided the dynamic mode as a simulation of a filter in the end of a tap sink. We created a continuous slow flow from the bottom to the top of the chamber and we performed an experiment set for 12 hours. We collected samples from outflow fluid every 10 minutes with in situ conductivity measurements (tables in appendix).

The frequency range was from 0.01 Hz-10000Hz for biochar concentration 10% and 20% and from 0.1Hz-10000Hz.for biochar concentration 100%

In semi-static mode, we also created continuous flow from the bottom to the top of the chamber but we stopped the flow in every measurement loop. So the RR120 water solution had a remain time to react with biochar in the chamber before collecting the outflow sample. After the sample collection at the end of the loop we continue the flow. The frequency range is exactly the same way as for the dynamic mode. Samples in both cases end up in chemistry laboratory for adsorption measurements.

resistance(Ohm)		100							
0,001405305									
resistance(Ohm)	resistivity (Ohm-m)	Fluid C (µS/cm)	- Phase (mrad)	Imag co	Real cond (S/m)	K	Imag (µS/cm)		
1946,2979	43,25106444	231,2081825	1,372	3E-05	0,023120796	246,2624	0,317217527		
1946,1932	43,24873778	231,2206209	0,884	2E-05	0,023122053	246,2757	0,204399002		
1946,0795	43,24621111	231,23413	0,558	1E-05	0,023123409	246,29	0,129028638		
1945,9697	43,24377111	231,2471772	0,358	8E-06	0,023124716	246,3039	0,082786488		
1945,8225	43,2405	231,2646709	0,227	5E-06	0,023126466	246,3226	0,05249708		
1945,7129	43,23806444	231,2776978	0,155	4E-06	0,023127769	246,3364	0,035848043		
1945,5849	43,23522	231,2929135	0,101	2E-06	0,023129291	246,3527	0,023360584		
1945,4563	43,23236222	231,3082026	0,084	2E-06	0,02313082	246,3689	0,019429889		
1945,3548	43,23010667	231,3202712	0,063	1E-06	0,023132027	246,3818	0,014573177		
1945,2623	43,22805111	231,3312709	0,055	1E-06	0,023133127	246,3935	0,01272322		
1945,1689	43,22597556	231,3423785	0,054	1E-06	0,023134238	246,4053	0,012492488		
1945,0922	43,22427111	231,351501	0,055	1E-06	0,02313515	246,4151	0,012724333		
1944,9961	43,22213556	231,3629318	0,046	1E-06	0,023136293	246,4272	0,010642695		
1944,8874	43,21972	231,3758627	0,045	1E-06	0,023137586	246,441	0,010411914		
1944,7781	43,21729111	231,3888664	0,047	1E-06	0,023138887	246,4549	0,010875277		
1944,6551	43,21455778	231,4035018	0,023	5E-07	0,02314035	246,4704	0,005322281		
1944,4722	43,21049333	231,425268	0,017	4E-07	0,023142527	246,4936	0,00393423		
1944,1899	43,20422	231,4588714	0,035	8E-07	0,023145887	246,5294	0,00810106		
1943,9202	43,19822667	231,490984	0	0	0,023149098	246,5636	0,001		
1943,3721	43,18604667	231,5562727	0,026	6E-07	0,023155627	246,6332	0,006020463		
1942,5668	43,16815111	231,6522654	0,029	7E-07	0,023165227	246,7354	0,006717916		
1945,039667	43,2231037	231,3577495		AVE	0,023135778	246,4218			



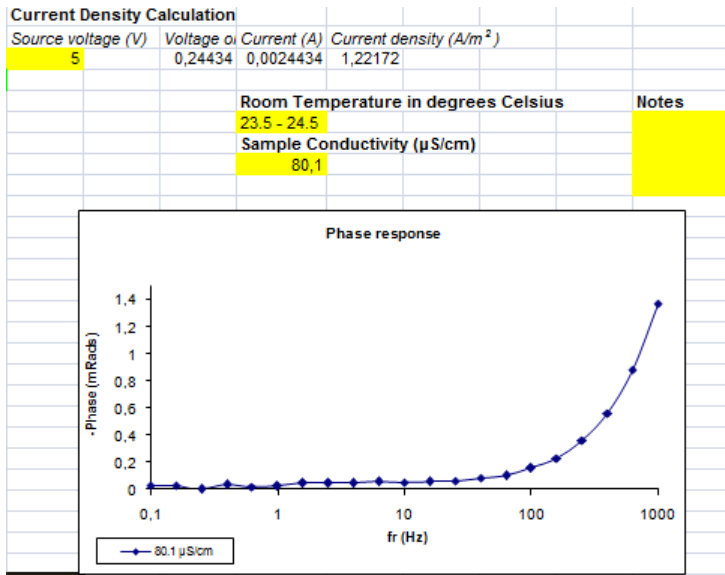


Figure 4.4 The collected raw data and a preliminary processing are shown.

5. Chemical Analysis

During the geophysical measurements, we took samples of the fluid and at the same time in the laboratory of chemistry, we measured the adsorption in the spectrophotometer. The Reactive dye (RR120, Sigma Aldrich) is detectable in $\lambda_{\max}=535\text{nm}$.

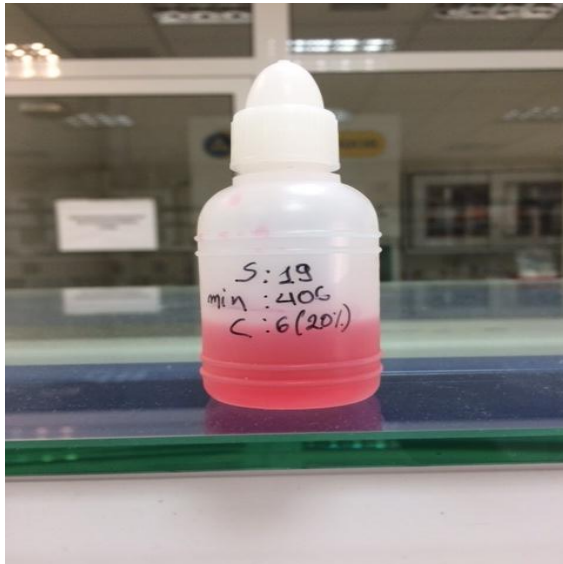


Figure 5.1 Typical samples from the experimental outflow.



Figure 5.2. UV mini 1240, UV-VIS spectrophotometer. SHIMADZU
 (https://www.google.gr/url?sa=t&rct=j&q=&esrc=s&source=web&cd=2&cad=rja&uact=8&ved=0ahUKEwjn4Z3Nq7rUAhVDAcAKHcSxACEQFggUAE&url=http%3A%2F%2Fwww.ssi.shimadzu.com%2Fproducts%2Fproduct.cfm%3Fproduct%3Duvmini&usg=AFQjCNEq44TvMpYfLP062K34Z0P_WITAYw)

5.1 RR120 Calibration of spectrophotometer

Before starting chemical analysis it was necessary to calibrate the instrument with the solution we were going to use in a range of concentration. The calibration curve was made with five standard RR120 solutions of different concentrations (10, 20, 50, 80, 100 mg/L).

Calibration tables and Curves

Table 5.1 Absorbance results for RR120 ($\lambda=535\text{nm}$) Columns C1-C5

absorbance	mg/L (ppm)
0,211	10
0,424	20
1	50
1,691	80
2,052	100

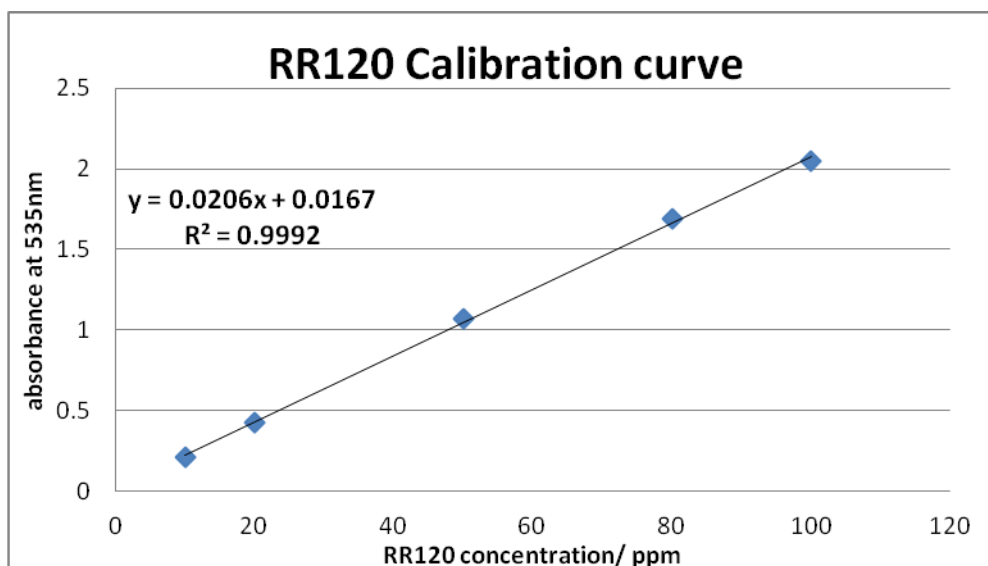


Figure5.3 Calibration curve for the RR120 aqueous solution. (Columns C1-C5)

Table 5.2 Absorbance results for RR120 ($\lambda=535\text{nm}$) (Columns C6-C7)

absorbance	mg/L (ppm)
0,211	10
0,424	20
1	50
1,691	80
2,052	100

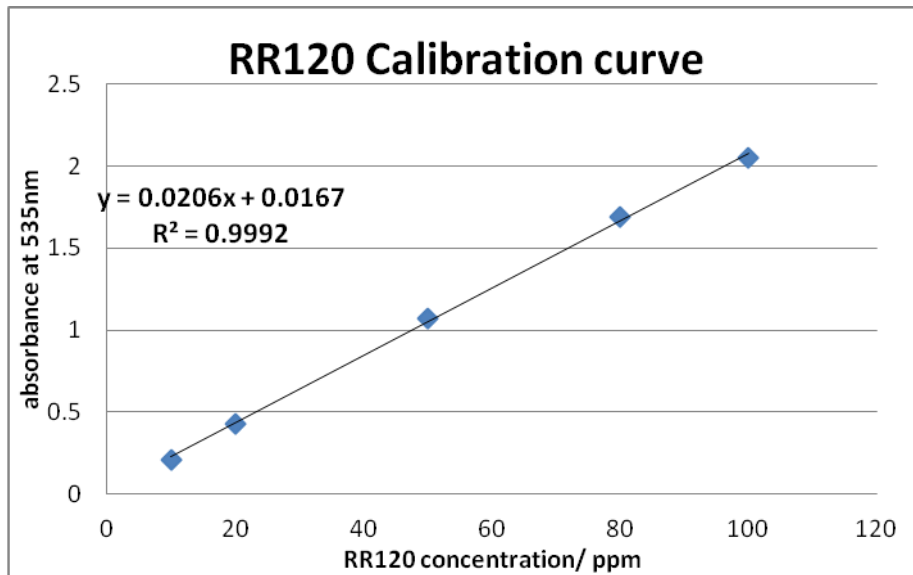


Figure 5.4 Calibration curve for the RR120 aqueous solution. (Columns C6-C7)

5.2 Adsorption results

Tables 5.3 Results of the adsorption for all the columns used.

10% biochar- column 5			Column 6 – SemiStatic(20%biochar)		
absorbance	concentration	Time (min)	absorbance	concentration (mg/L)	time (min)
1,764	84,82038835	56	1,479	70,98543689	36
1,911	91,95631068	105	1,322	63,36407767	75
1,901	91,47087379	150	1,612	77,44174757	112
1,856	89,28640777	190	1,769	85,0631068	148
1,818	87,44174757	230	1,849	88,94660194	183
1,771	85,16019417	280	1,891	90,98543689	220
1,817	87,39320388	334	1,941	93,41262136	256
1,917	92,24757282	379	1,924	92,58737864	295
1,926	92,68446602	416	1,924	92,58737864	329
1,92	92,39320388	456	1,955	94,09223301	365
1,965	94,5776699	498	1,998	96,17961165	406
1,965	94,5776699	550	2,018	97,15048544	457
1,975	95,0631068	587	2,046	98,50970874	494
1,938	93,26699029	631	2,018	97,15048544	536
1,943	93,50970874	672	2,046	98,50970874	550
1,96	94,33495146	740	2,032	97,83009709	600

Column 7 - Dynamic		
absorbance	concentration	time (min)
1,299	62,24757282	55
1,574	75,59708738	95
1,877	90,30582524	127
1,913	92,05339806	167
1,941	93,41262136	210
1,935	93,12135922	259
1,886	90,74271845	315
1,891	90,98543689	354
1,992	95,88834951	420
2,025	97,49029126	460
2,032	97,83009709	499
2,046	98,50970874	544

Reference – column 1		
Time (min)	absorbance	Concentration (mg/L)
56	1,944	93,55825243
105	1,992	95,88834951
150	1,992	95,88834951
190	1,971	94,86893204
230	1,959	94,28640777
280	1,965	94,5776699
334	1,959	94,28640777
379	1,975	95,0631068
416	1,975	95,0631068
456	1,935	93,12135922
498	1,975	95,0631068
550	1,975	95,0631068
587	1,975	95,0631068

Column 2- 100% biochar		
time/min	absorbance	RR120 concentration
1	0,093	3,703883495
3	0,206	9,189320388
5	0,241	10,88834951
12	0,393	18,26699029
17	0,486	22,7815534
24	0,484	22,68446602
33	0,353	16,32524272
42	0,327	15,0631068
52	0,311	14,28640777
61	0,307	14,09223301
72	0,339	15,64563107
84	0,337	15,54854369
95	0,356	16,47087379
100	0,379	17,58737864
110	0,51	23,94660194

5.3 Adsorption curves

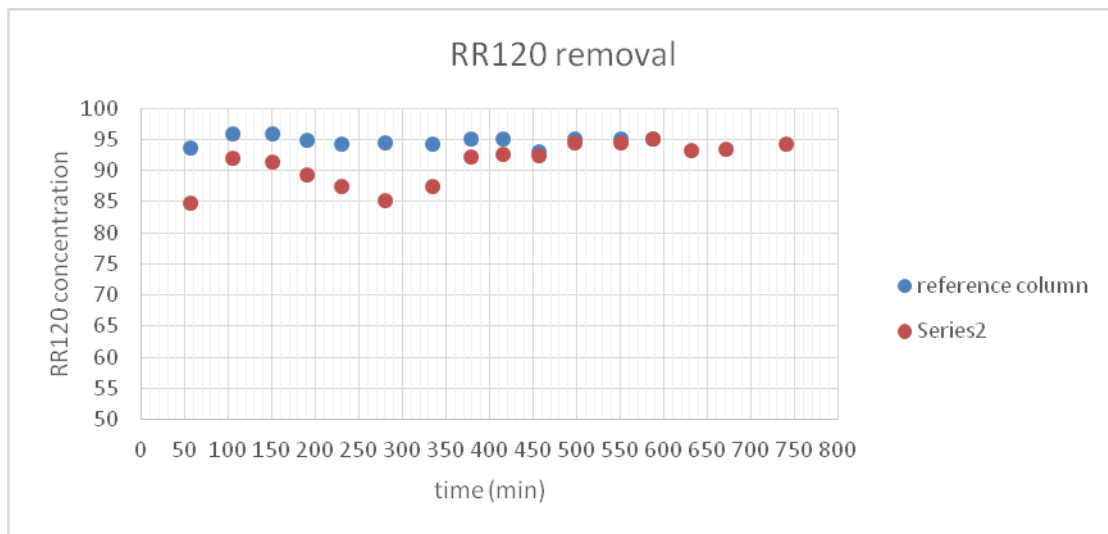


Figure 5.5 Column 1(reference) - column 5(10% biochar)

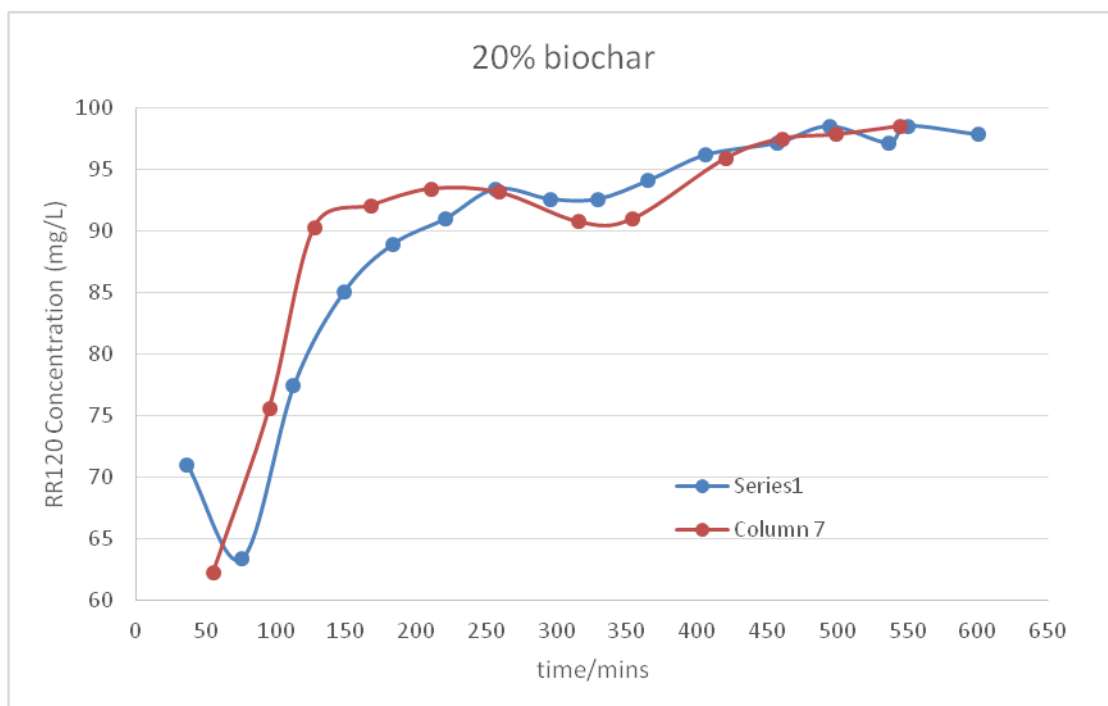


Figure 5.6 Column 6- column 7 (20% biochar)

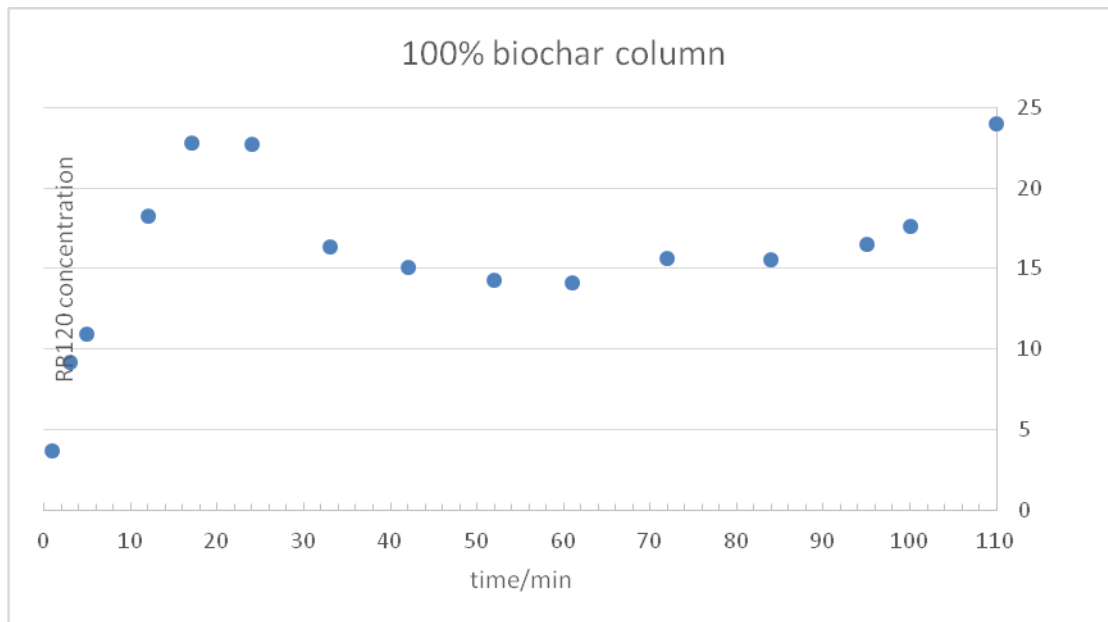


Figure 5.7 Column 2 (100% biochar)

6. RESULTS

In this chapter, we present the processed preliminary results for all the used columns in two different electrode combinations for each column. The distance between P1-P5 is 0.12m and between P2-P4 is 0.06m. For every column we have results from 24 loops except column 2 and we export diagrams for phase response, real and imaginary conductivity for the two different electrode combinations. To end up in the preliminary results we show frequency, magnitude and phase shift graphs.

Column 1(reference)

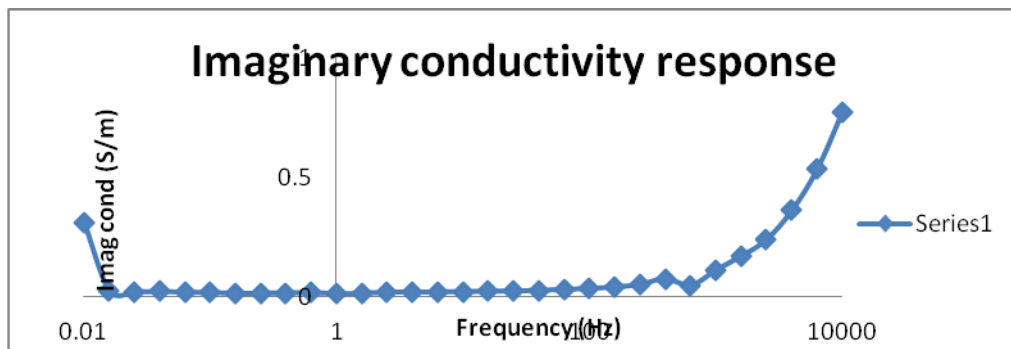
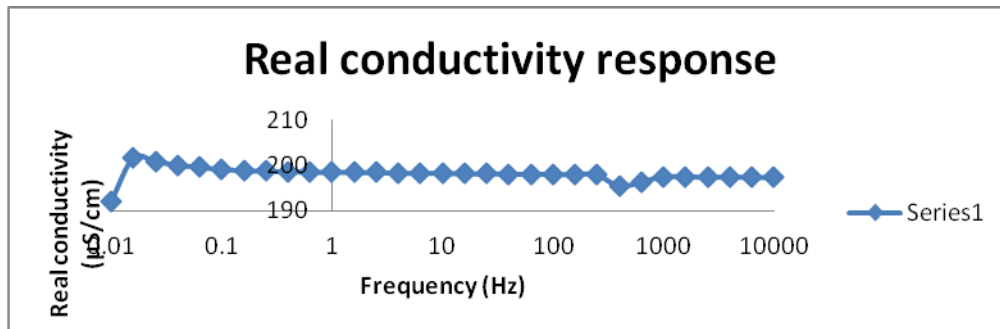
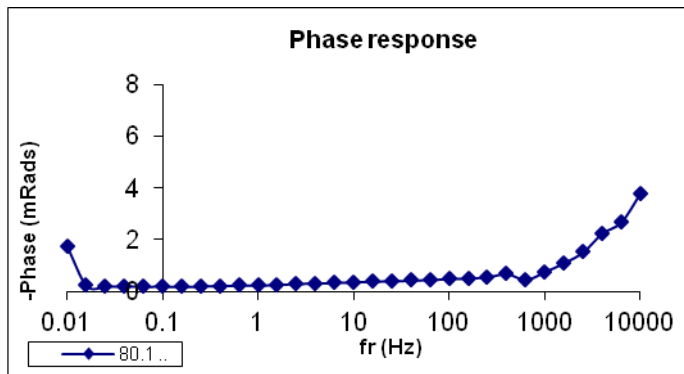
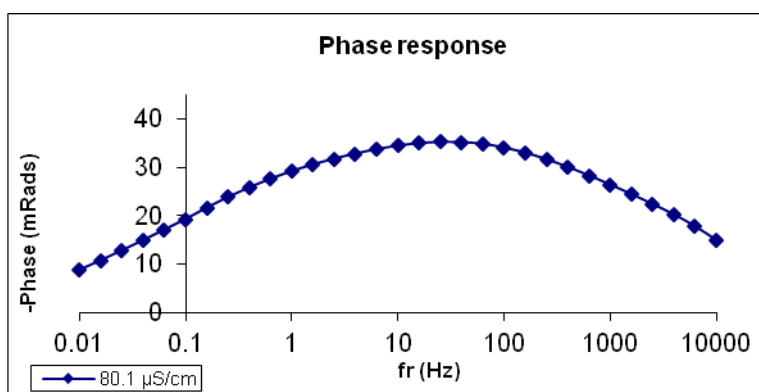


Figure 6.1 Phase, imaginary and real conductivity for column 1 and P1-P5 electrode combination.

Column 5(10%biochar)



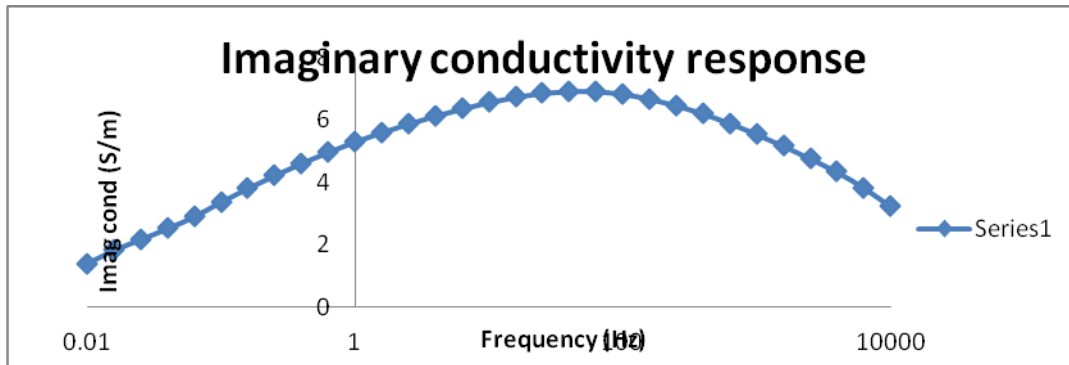
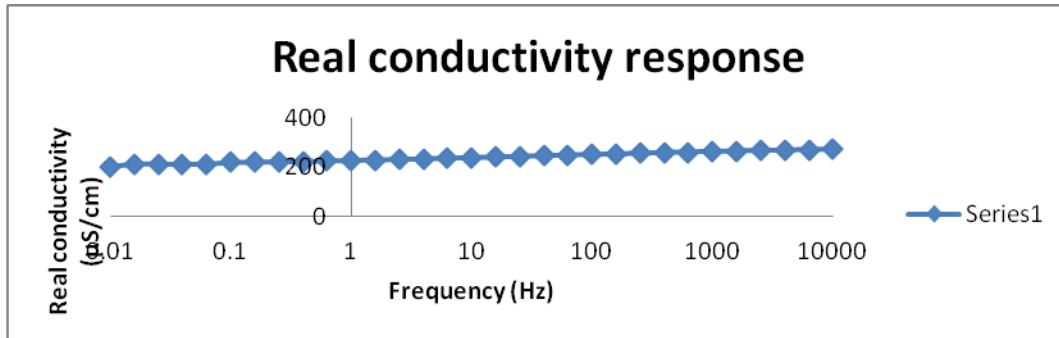
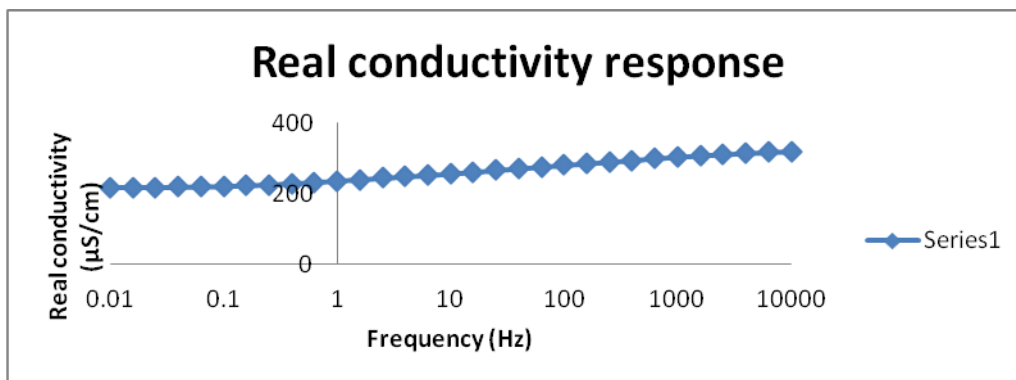
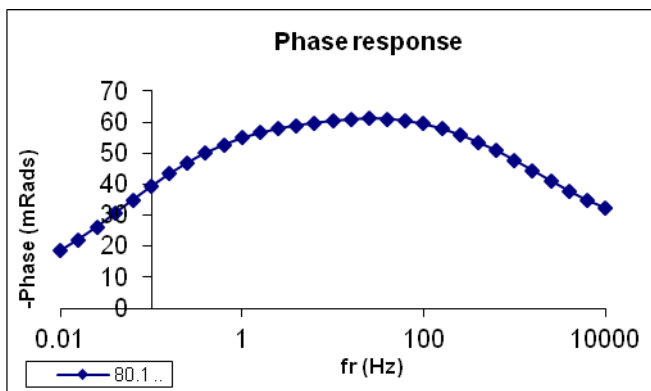


Figure 6.2 Phase, imaginary and real conductivity for column 5 and P1-P5 electrode combination.

Column 6(20%biochar)



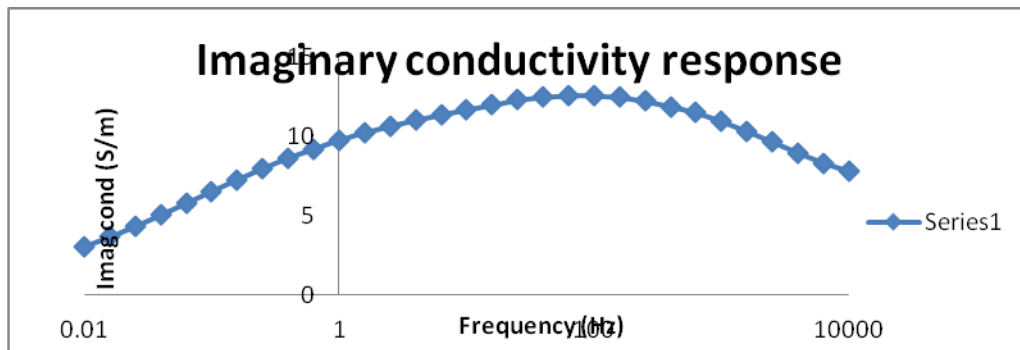
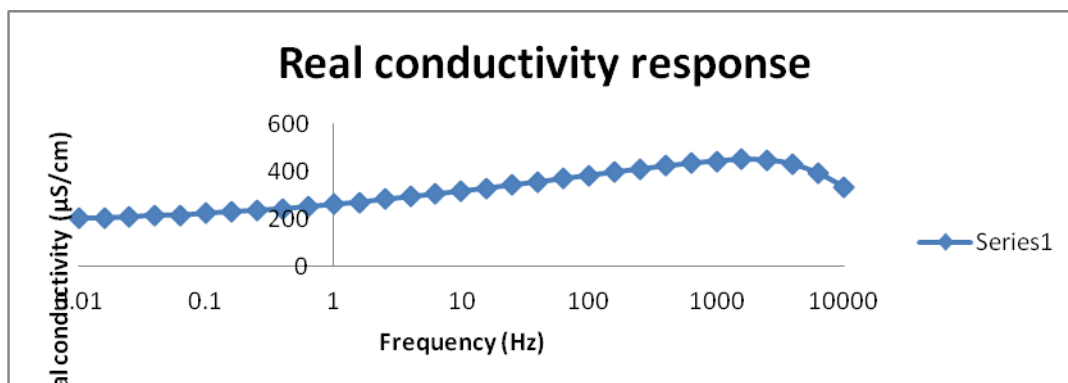
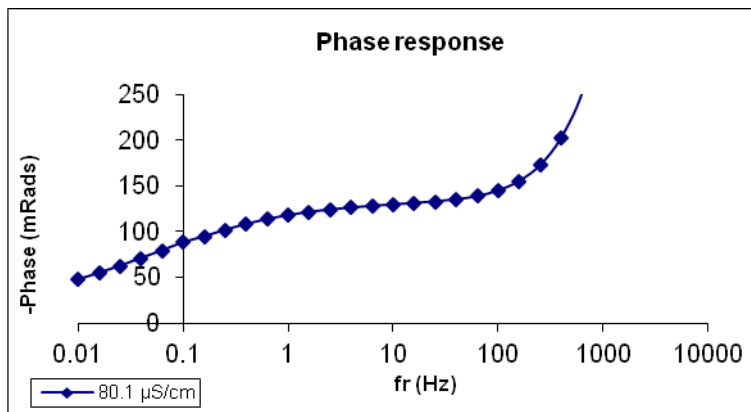


Figure 6.3 Phase, imaginary and real conductivity for column 6 and P1-P5 electrode combination.

Column 7(20%biochar)



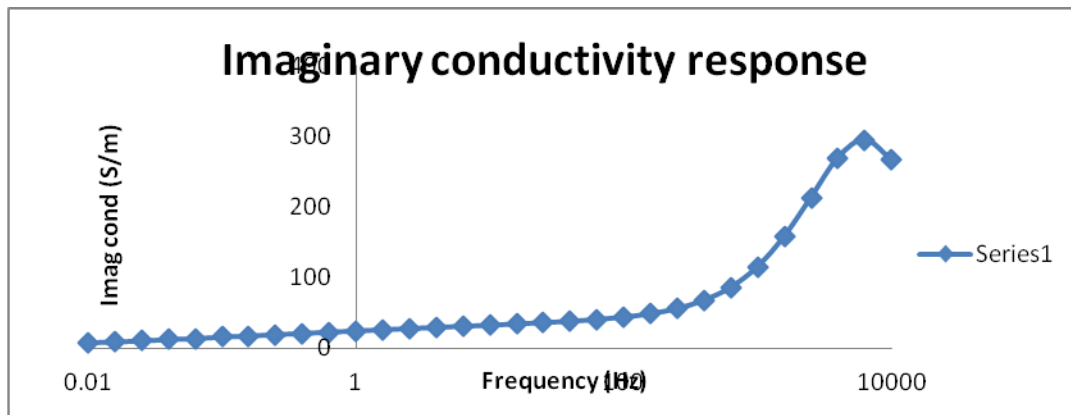
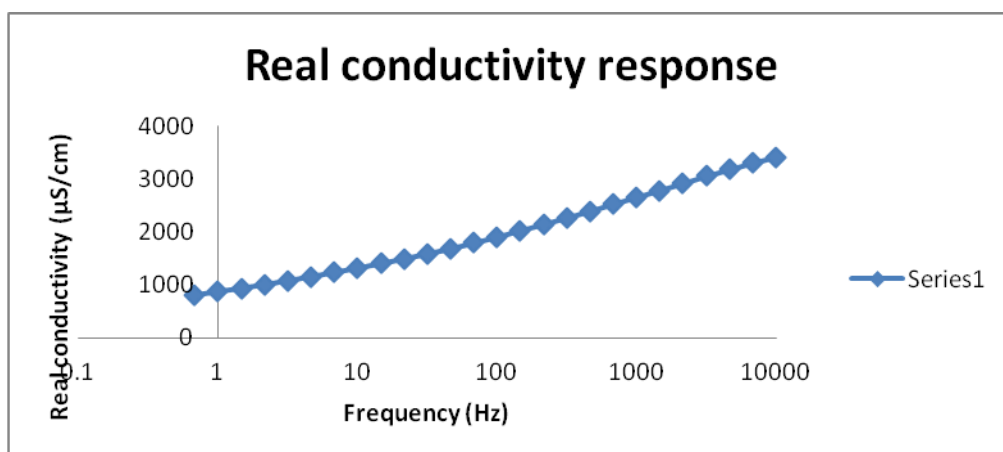
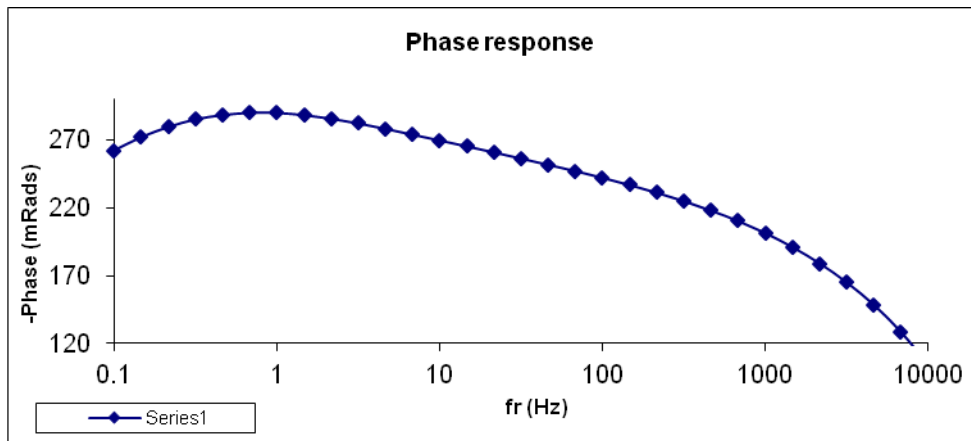


Figure 6.4 Phase, imaginary and real conductivity for column 7 and P2-P4 electrode combination.

Column 2
(100%biochar)



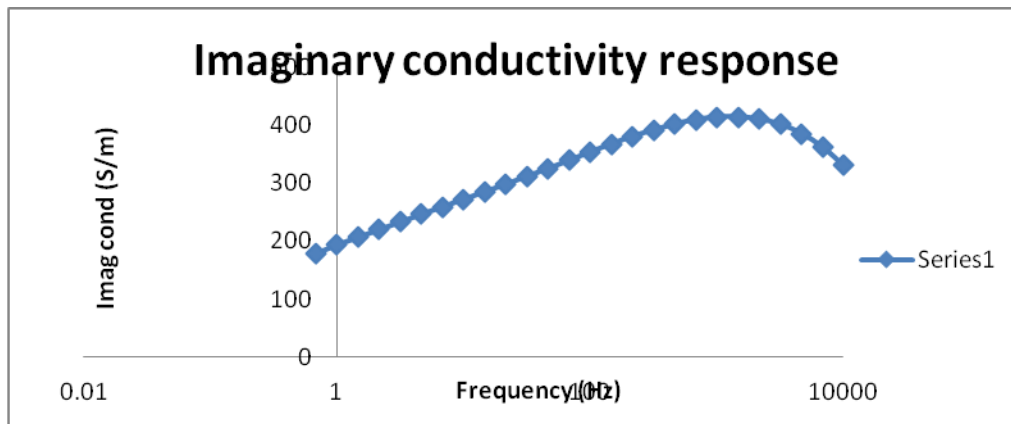
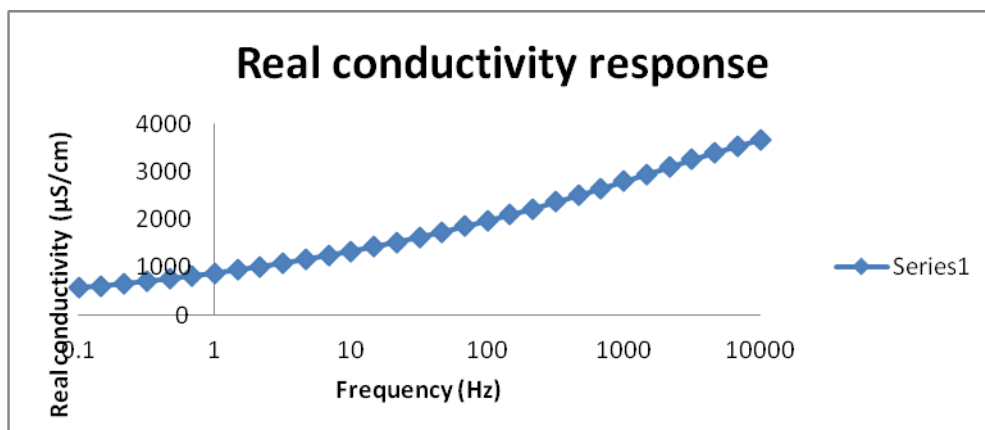
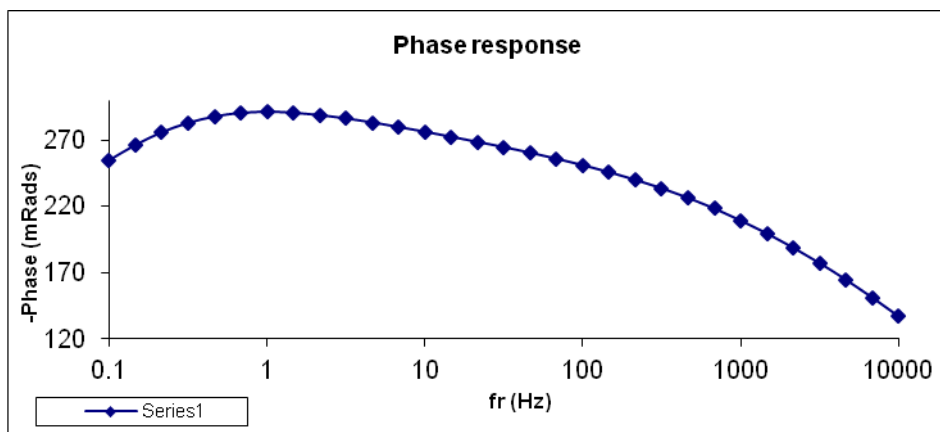


Figure 6.5 Phase, imaginary and real conductivity for column 7(100%biochar and dionised water) and P2-P4 electrode combination. For the experiment with dionised water we had 12 loops.



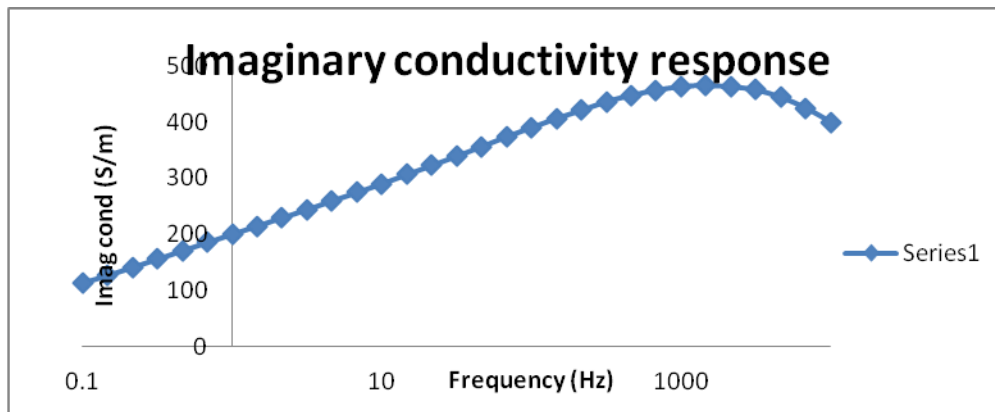


Figure 6.6 Phase, imaginary and real conductivity for column 7(100%biochar and RR120) and P2-P4 electrode combination. For the experiment with RR120 we had 15 loops.

More diagrams for different combinations in another loop of a column are given in the appendix.

7. Interpretation

Qualitative and not quantitative interpretation was performed due to limited knowledge on how the decontamination process is working. For an integrated view regarding the chemical mechanism and its SIP response we suggest combined geophysical and geochemical analysis.

7.1 SIP Interpretation

Results of the use of the SIP method are presented. The first diagram concerns the frequency IP response and the accuracy of the SIP instrument. The phase sensitivity of the instrument according to the manufacturers is 0.5mrad. In the diagram below the phase ranges from 4-12 mrad for all frequencies and exceed the sensitivity of the instrument. The diagram below describes the phase for different frequencies and all the loops. The colored lines denote different loops. Within the circle we observe a peak frequency shift, which is an indication of the degradation procedure.

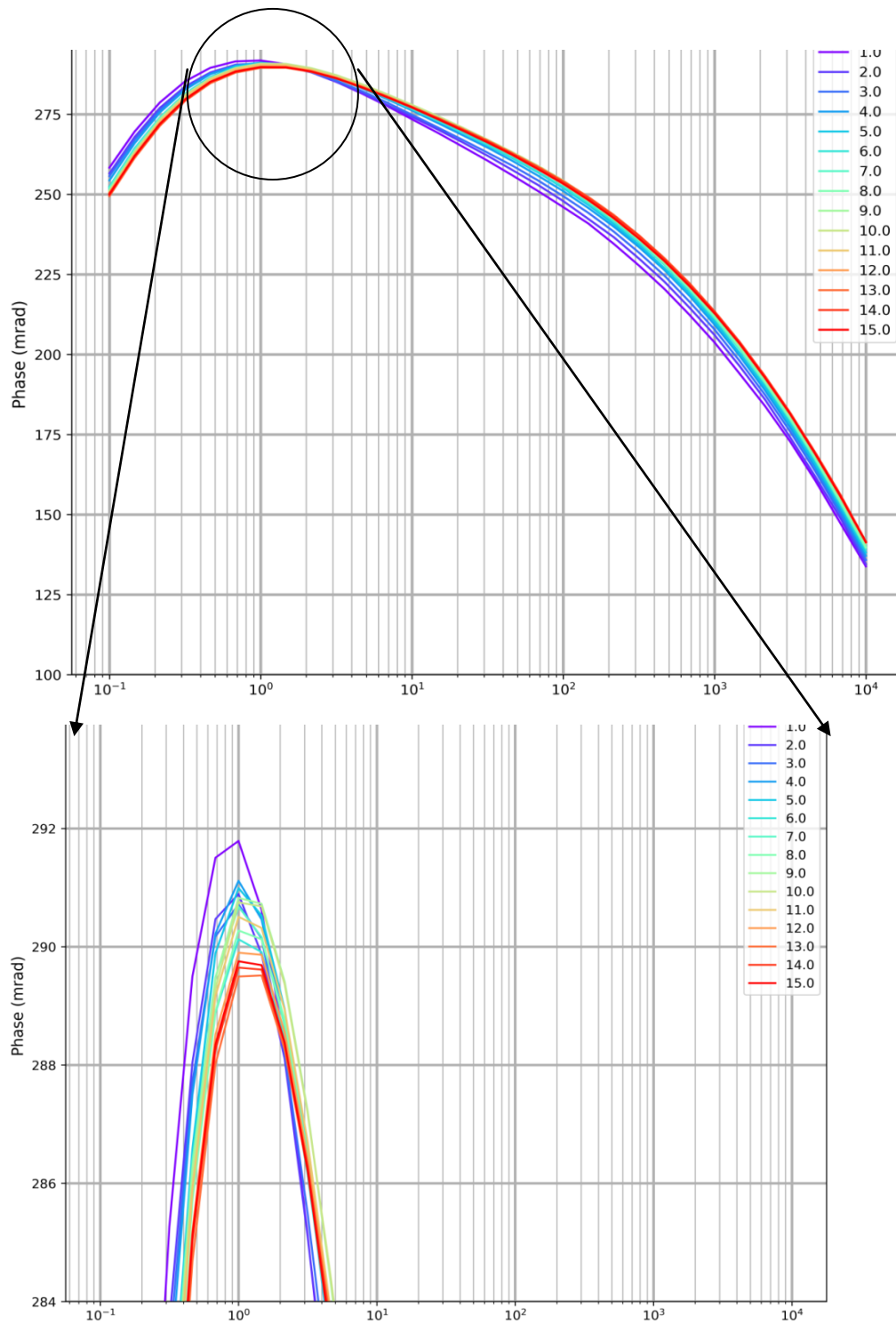
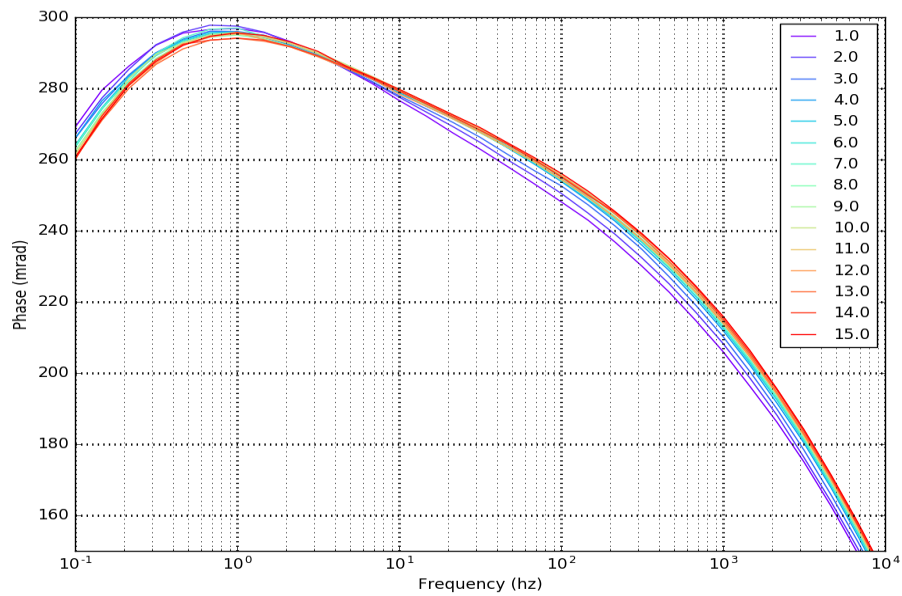


Figure 7.1 Temporal evolution for column 20% biochar+RR120. Peak frequency shifts towards higher frequencies. Average peak frequency 0.7Hz. The phase follows the degradation procedure.

Next we compare measurements for RR120 and dionised water (Fig. 7.2). From the results, it is clear that the mentioned above SIP signal is recorded only when the column is filled with TW. Namely, there is a peak frequency change in the RR120 diagram and no change in the dionised water diagram. It clearly shows that the SIP method responds when we use a

conductive fluid. During the measurements using the TWW, the adsorption mechanism is in progress as remediation process and it can be detected. The peak frequencies at RR diagram is time dependent. The peak frequency occurs in a range of frequencies and for every peak frequency we can detect different phase of the chemical procedure.

RR120



Dionised water

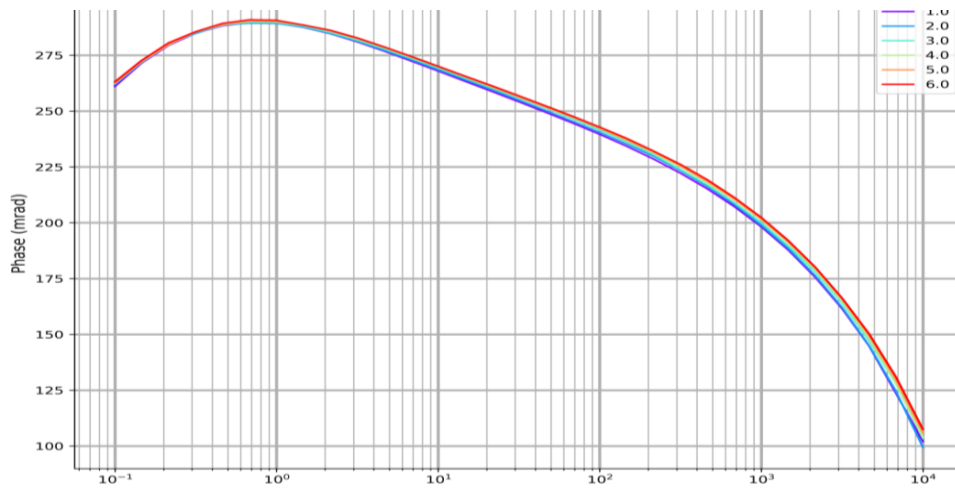


Figure 7.2. Phase versus frequency diagrams show that there is a phase change in the RR120 diagram and no change in the water diagram..

In the diagrams below we show resistivity, phase, real and imaginary conductivity as a function of time or iteration for selected frequencies. Red line corresponds to RR120 and blue line, to the water. We chose peak frequency at 1Hz because this is the peak frequency for the 100% biochar experiment, where the column was either filled with dionised water or TWW.

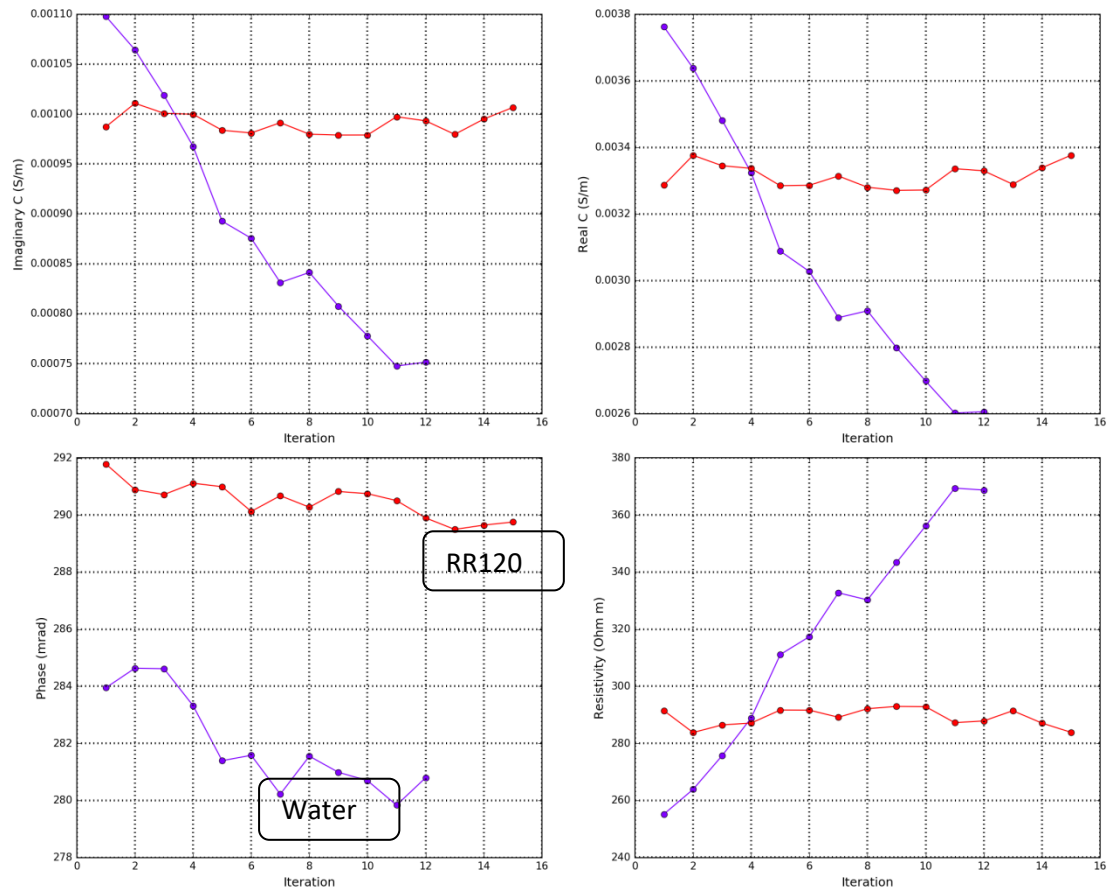


Figure 7.3 Column 100% biochar (RR & Water)-imaginary & real conductivity, phase and resistivity change at 1Hz. Clearly different phase magnitude and distinctively different trends.

Then, a dominant frequency (63Hz) was selected from the column with 10% biochar and we observe phase changes with the iteration. In every data set we chose the frequency with the clearest frequency trend.

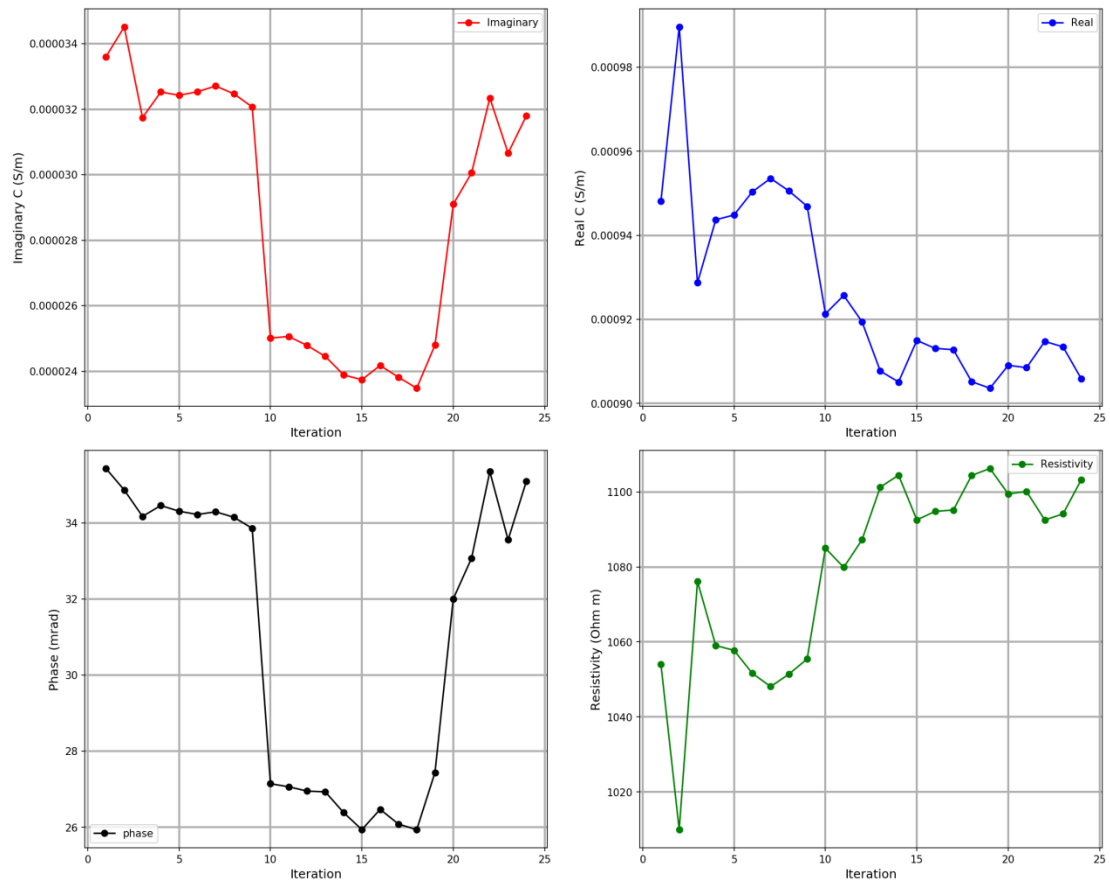


Figure 7.4 10% Biochar, Phase, Imaginary & Real conductivity, Resistivity change at PF: 63Hz.

7.1.1 Frequency dependence

From the results so far we conclude that the degradation process is a frequency dependent phenomenon. We are going to present diagrams for column 2 with 100% biochar which show how phase changes in a range of frequencies for dionised water and RR120. There is distinct diversification for the SIP signal between the two fluids.

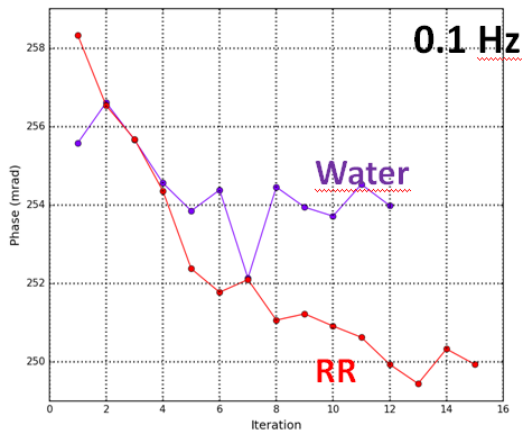
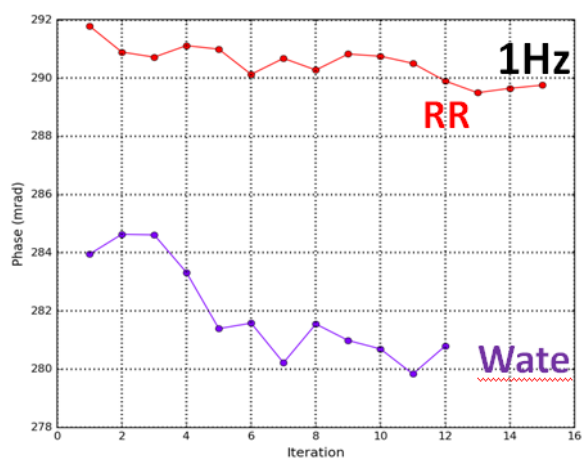
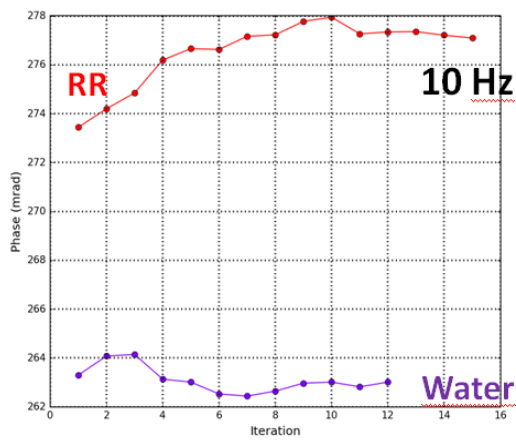
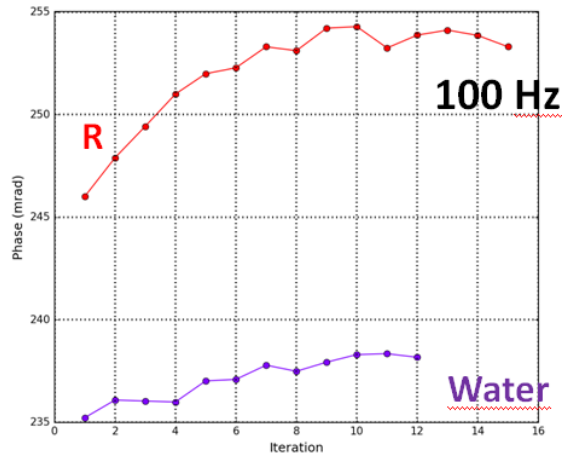
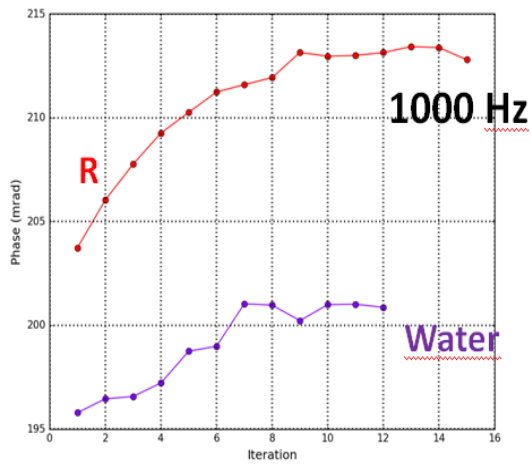


Figure 7.5 Diagrams for five selected frequencies for column 2 (100% biochar) .Blue lines is the response for dionised water and red line for RR120.

For selected frequencies we observe different phase trend for water and RR solution.

7.2.2 Comparison geophysics vs geochemical

A consistency between the geophysical monitoring and the geochemical analysis was observed. The next diagram describes the dynamic condition for 10% biochar and RR120 namely we present phase and RR concentration as a function of time (iteration) in the case of a constant fluid flow. The red line shows the RR concentration, the black line the SIP signal and the dashed line is the running average of the latter. Within the dashed ellipse there is an agreement between geophysical and geochemical measurements, namely both techniques encounter the maximum change during this time period.

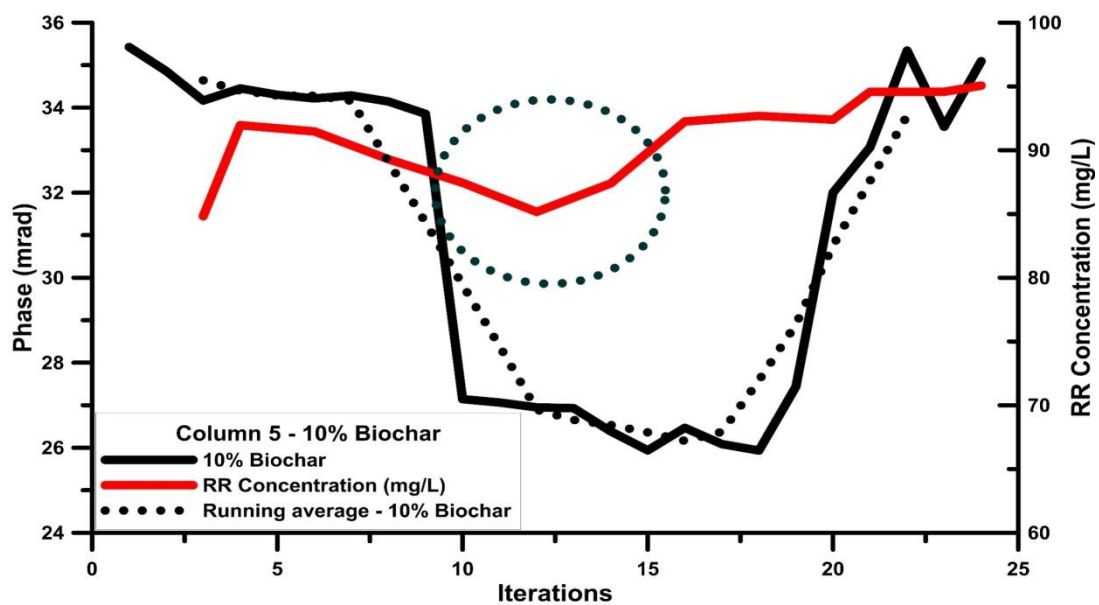


Figure 7.10 Integration of geophysical measurements with geochemical analysis Ellipse spotted the time that, we observed the maximum change of the phase and RR concentration.

In the diagrams below for column 6 (20% biochar) and both modes (semi static and dynamic) we have even more encouraging results. The difference was in the biochar mixture, we had larger compared to column 5 biochar concentration so bigger adsorption ability. We present phase and concentration with time in minutes. The red line is RR concentration, the black is the SIP signal and the dashed line is the runnings average for the SIP. From the graphs, we conclude that we can detect with the SIP method the chemical procedure. This diagram shows clearly that the fluid starts to saturate the chamber, then it comes in a balance with the biochar mixture after 150minutes and then adsorption procedure starts. In the dashed

ellipse is the point that is the maximum of the phase change and the point that we have the maximum adsorption. After 400 minutes it seems to reach equilibrium and the inflow fluid it is outflow as well. The peak frequency for the semi static mode was 10Hz and for dynamic mode 1Hz. From the experiment with the two different flow conditions we conclude that the remain time of the fluid in the chamber in reaction with biochar does not affect the sorption mechanism. Biochar has a specific area which can adsorb particular amount of the contaminant, when the specific area of the grains is full of the chemical groups it can absorb, the procedure stops.

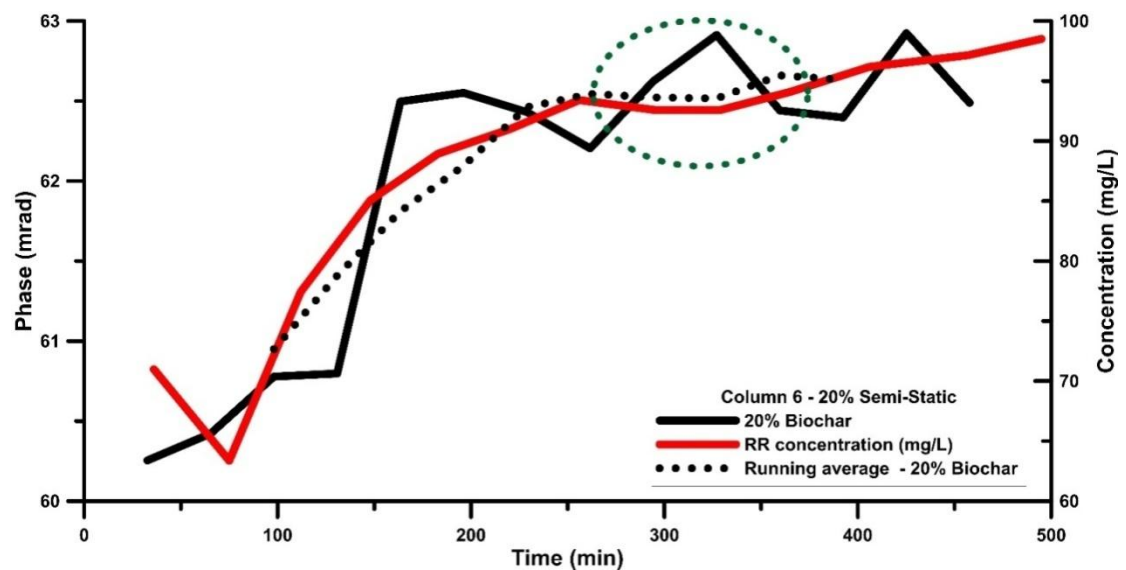


Figure 7.11 Temporal evolution of the phase magnitude. The phase shift follows contaminant concentration decrease. Semi static. (10Hz)

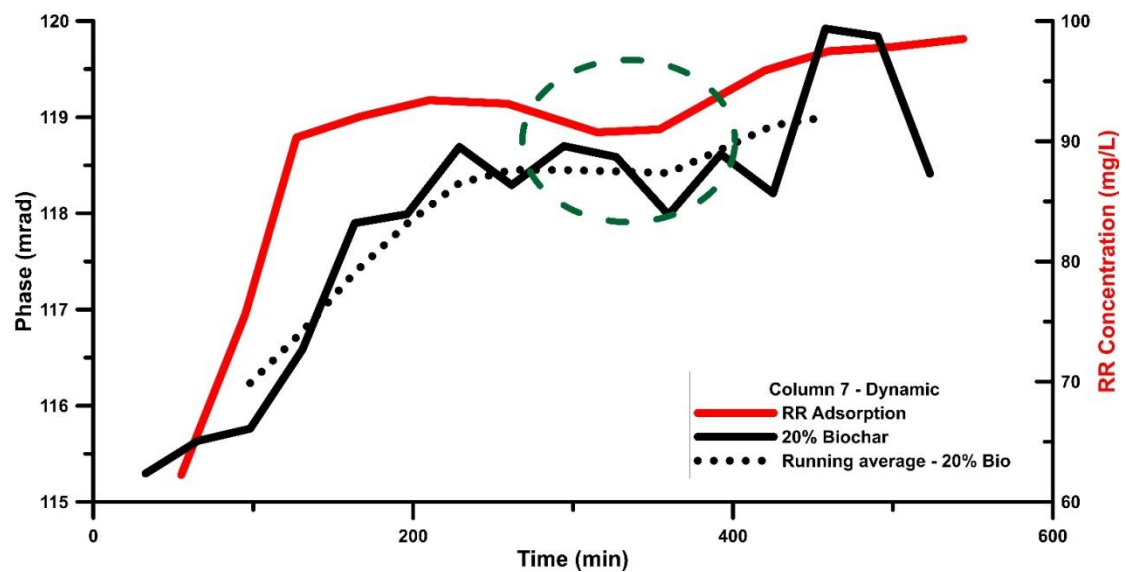


Figure 7.12 Temporal evolution of the phase magnitude. The phase shift follows contaminant concentration decrease. Dynamic mode. (1Hz)

Next diagram shows results from the experiment with 100% biochar in dynamic mode for peak frequency of 1Hz. Although we achieved maximum adsorption, the SIP signal was not so clear. In the figure 7.13, we present the temporal evolution for the phase magnitude. In this diagram, we can see the different trends for the two fluids, the conductive and the deionised water. The maximum adsorption at a rate almost 85% at 250 min to 450 min does not agree with the recorded phase from the geophysical method. In order to explain this observation we propose the application of geophysical data processing techniques such as Debye decomposition as well as FTIR analysis of existing samples from the inner of the chamber as well.

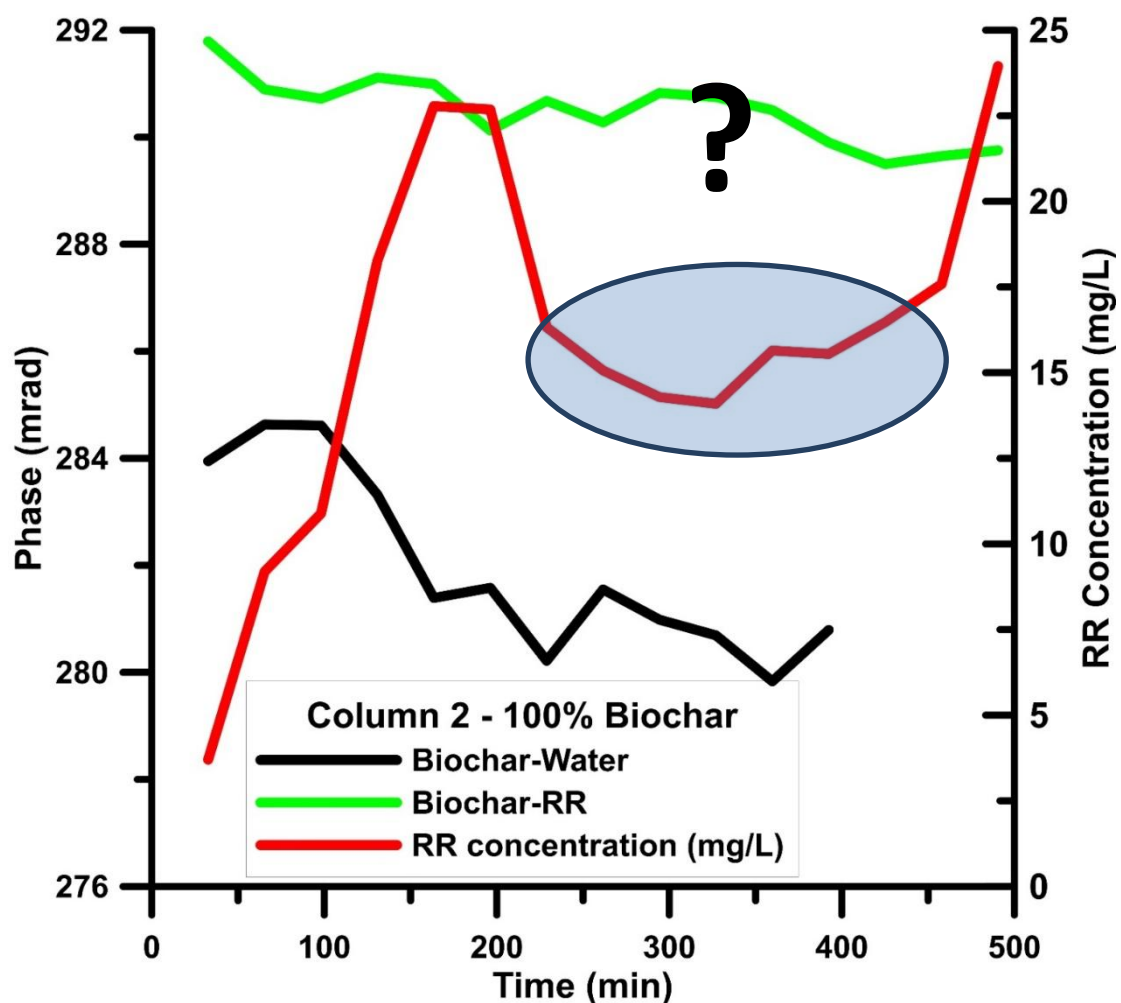


Figure 7.13 Temporal evolution of phase magnitude for 100% biochar (content). Dynamic mode in peak frequency 1Hz.

We achieved maximum adsorption and TWW decoloration after 20 minutes in dynamic mode (Fig 7.14). Even for a short remaining time of the TWW in the chamber, the decoloration was achieved.



Figure 7.14 TWW before and after treatment.

8. Conclusions

The SIP method can be a reliable tool for monitoring inorganic contaminant. It has the ability to take measurements in a wide range of frequencies so it is possible to can detect inorganic or anorganics contaminants.

From the calibration measurements we notice that the method is sensitive to conductive and resistive fluids which encounter small deviations in dissolved particles concentration.

Biochar was successful in removing the RR120 from the aqueous solution. Chemical analysis showed that a considerable amount of the wastewater adsorbed on biochar. Table 8.1 shows that the adsorption is directly related to biochar's concentration in the column, and flow conditions do not affect the reaction.

Table 8.1 Contaminant removals in percentage are depended on biochar's amount in the chambers.

Biochar concentration	Adsorption
10 %	16 %
20 % - semi static	37 %
20 % - dynamic	38 %
100 %	84 %

According to the presented experiments, there is consistency between the measurements, indicating that the results are reliable. A similar trend with a constant drift is observed in phase-time diagrams for water and the TWW the phase being larger for TWW. TWW response has been detected, and is characterized by a strong spectral signature.

Very significant conclusion for the TWW/dionised water comparison is that water resistivity increases with time while TWW resistivity decreases with time. Thus geoelectrical behavior appears to be different between dionised water and TWW.

Increasing biochar's concentration in the chamber, the adsorption ability increases too, but there was no difference in adsorption's ability for dynamic or semi-static mode conditions.

The experiments presented here showed that the SIP method is a potential monitoring tool for remediation processes.

References

- Atekwana E, Slater L, Estella A. 2009, Full publication history; DOI: 10.1029/2009RG000285
- Abdel A, Atekwana G. Z., Slater L, and. Atekwana E. A 2004, Effects of microbial processes on electrolytic and interfacial electrical properties of unconsolidated sediments, *Geophysics. Res. Lett.*, 31, L12505, doi: 10.1029/2004GL020030
- Agrafioti A, Kalderis, Diamadopoulos 2014 - *Journal of environmental*, Elsevier. This work investigated the production of Ca and Fe modified biochars in order to use them for the removal of arsenic As (V) and chromium Cr (VI) from aqueous solutions.
- Arica M. Yakup, Gülay Bayramoğlu 2007, Biosorption of Reactive Red-120 dye from aqueous solution by native and modified fungus biomass preparations of *Lentinus sajor-caju* *Journal of Hazardous Materials*. Volume 149, Issue 2, 22 October 2007, Pages 499–507
- Benson et al. 1984. *Groundwater Geophysics in Hard Rock* National Academy Press.
- Breede K, Kemna A., Esser O., Zimmerman E, Vereecken H., Huisman J.A, 2010. Joint Measurement Setup for Determining Spectral Induced Polarization and Soil Hydraulic Properties .
- Cartwright and McComas 1968, Warner 1969, Stoller and Roux 1973, Klefstad 1975, Barker 1990, Ross et al.1990, Carpenter et al. 1990, Naudet et al. 2003,2004)
- Chen and Chen 2009. Sorption of naphthalene and 1-naphthol by biochars of orange peels with different pyrolytic temperatures. *Chemosphere*, Elsevier.
- Daskalaki Vasileia M., Eleni S. Timotheatou, Alexandros Katsaounis, Dimitrios Kalderis 2011, Degradation of Reactive Red 120 using hydrogen peroxide in subcritical water. Volume Pages 200–205
- Gurnham 1965, *Industrial wastewater control*, Editor, Academic Press, New York (1965), 476 pages. RD Hoak - *AIChE Journal*, 1965 - Wiley Online Library
- Gawel B. 2016, *Gas adsorption: Study of the porosity of materials*. Norwegian University of science and technology (NTNU)
- Joyce 2012, Sensitivity of spectral induced polarization measurements to environmental contaminants (nanoparticles and hydrocarbons) RA Joyce - 2012 - shareok.org
- Kemna Andreas, Andrew Binley, Giorgio Cassiani, Ernst Niederleithinger, Andre Revil, Lee Slater, Kenneth H. Williams, Adrian Flores Oroxco, Franz-Hubert Haegel, Andreas Hordt, Sabine Kruschwitz, Virginie Leroux, Konstantin Titov and Egon Zimmerman 2012, An overview of the spectral induced polarization method for near-surface applications. *Near Surface Geophysics*, 10(6):453-468.
- Karakoyun N, Senol Kubilay, Nahit Aktas, Omer Turhan, Murat Kasimoglu, Selahattin Yilmaz, Nurettin Sahiner 2011, Hydrogel–Biochar composites for effective organic contaminant removal from aqueous media. Pages 319–325

Kasozi et al. 2010, Catechol and Humic Acid Sorption onto a Range of Laboratory-Produced Black Carbons (Biochars)

Department of Geological Sciences, University of Florida, 241 Williamson Hall, Gainesville, Florida 32611-2120, Department of Soil and Water Science, University of Florida, Gainesville, Florida, and Department of Agricultural and Biological Engineering, University of Florida, and Gainesville, Florida Environ. Sci. Technol., 2010, 44 (16), pp 6189–6195

Kusvuran E, Gulnaz O, Irmak S, Atanur OM, Yavuz HI, Erbatur O. 2004, Comparison of several advanced oxidation processes for the decolorization of Reactive Red 120 azo dye in aqueous solution. 109 (1-3):85-93.

Kirmizakis, P., 2016, Laboratory scale application of spectral induced polarization (SIP) method for environmental monitoring, MSc thesis, Technological Educational Institute of Crete, pp. 124.

Lanz Eva, Hansruedi Maurer, and Alan G. Green 1998. "Refraction tomography over a buried waste disposal site." *Geophysics* 63, special section: shallow seismic reflection. *Papers*, 1414-1433. doi: 10.1190/1.1444443

Lesmes David P. and Kevin M. Frye, 2001. *Papers on Chemistry and Physics of Minerals and Rocks Volcanology. Influence of pore fluid chemistry on the complex conductivity and induced polarization responses of Berea sandstone.* Wiley Online Library

Leroy and Revil 2009. Spectral induced polarization of clays and clay-rocks. Research Gate

Leroy P., Revil, A., Kemna, A., Cosenza, P., & Ghorbani, A. 2008, Complex conductivity of water-saturated packs of glass beads. *Journal of Colloid and Interface Science*, 321(1), 103–117. <http://doi.org/10.1016/j.jcis.2007.12.031>

Lin and Lin 1992, Environmental systems. Decolorization of textile effluents by ozonation. Department of Chemical Engineering Yuan Ze Institute of Technology, Taiwan. Vol. 21(2) 143-156, 1991-92.

Nguyen F., Kemna, A., Antonsson, A., Engesgaard, P., Kuras, O., Ogilvy, R. Pulido-Bosch A. 2009. Characterization of seawater intrusion using 2D electrical imaging. *Near Surface Geophysics*, 7(5-6), 377–390. <http://doi.org/10.3997/1873-0604.2009025>

Ntarlagiannis D. 2006. *Investigating Geophysical Signatures of Microbial Cells, Processes, and Degradation: Implications for the Geophysical Monitoring of Microbial Activity and Degradation in the Subsurface.* Rutgers University (State University of New Jersey), USA.

Ntarlagiannis, D., & Ferguson, A. 2009, SIP response of artificial biofilms. *Geophysics*, 74(1), 1–5. <http://doi.org/10.1190/1.3031514>

Parasnis, D. S. 1986, *Principles of Applied Geophysics (4th Edition).* 29 West 35th Street. New York. NY 10001: Chapman and Hall. <http://doi.org/10.1007/978-94-009-4113-7>

Ponziani M, Slob E.C., Vanhala H. and Ngan D.J.M -Tillard, 2011, International Water Technology Journal, IWTJ Vol. I - Issue 1, June 201114. Influence of water content on the electrical conductivity of peat.

Prodan C., F. Mayo, J. R. Claycomb, J. H. Miller, and M. J. Benedik 2004, Low-frequency, low-field dielectric spectroscopy of living cell suspensions. *Appl. Phys.*,95, 3754–3756.

Papazachos 1986, Introduction to applied geophysics.

Revil A., Karaoulis M., Johnson T., & Kemna A. 2012, Review: Some low-frequency electrical methods for subsurface characterization and monitoring in hydrogeology. *Hydrogeology Journal*, 20(4), 617–658. <http://doi.org/10.1007/s10040-011-0819-x>.

Reynolds J. M. 2011, An Introduction to Applied and Environmental Geophysics. *Geophysics* (2nd Edition, Vol. 1). <http://doi.org/10.1017/CBO9781107415324.004>.

Rattee and Stepheness 1956. Reactive dyes first appeared commercially in 1956, after their invention in 1954 at the Imperial Chemical Industry (ICI).

Robert 1989. *Geophysical Data Analysis: Discrete Inverse Theory*. pp. iii-xii, 1-285

Slater L, Ntarlagiannis D, Personna Y, Susan Hubbard, Hydrology and Land Surface Studies. Pore-scale spectral induced polarization signatures associated with FeS biomineral transformations. *Geophysical research Letters* 34 L21404. DOI: 10.1029/2007GL031840

Slater L. 2007, Near Surface Electrical Characterization of Hydraulic Conductivity: From Petrophysical Properties to Aquifer Geometries—A Review <http://link.springer.com/journal/10712>. Volume 28, Issue 2, pp 169–197

Slater L., Lesmes D. 2002, IP interpretation in environmental investigations. *Geophysics*, 67(1), 77. <http://doi.org/10.1190/1.1451353>

Sen P. N, Scala C, and M. H. Cohen 1981, "A self-similar model for sedimentary rocks with application to the dielectric constant of fused glass beads." *GEOPHYSICS*, 46(5), 781-795. doi: 10.1190/1.1441215

Spokas K ,Keri B. Cantrell, Jeffrey M. Novak, David W. Archer ,Ames A. Ippolito, Harold P. Collins ,Akwas A. Boateng, Isabel M. Lima, Marshall C. Lamb, Andrew J. McAloon, Rodrick D. Lentz and Kristine A. Nichols 2012 Biochar: A Synthesis of Its Agronomic Impact beyond Carbon Sequestration *Journal of Environmental Quality* doi:10.2134/jeq2011.0069

Soulios 1986, *General Hydrology*

Tsourlos P., Vargemezis G. N., Fikos I., Tsokas G. N. 2014, DC geoelectrical methods applied to landfill investigation: Case studies from Greece. *First Break*, 32(8), 81–89.

Ustra A, Slater L, Ntarlagiannis D ,Vagner E. 2012, Spectral Induced Polarization (SIP) signatures of clayey soils containing toluene. *Near Surface Geophysics*, 10(6), 503–515. <http://doi.org/10.3997/1873-0604.2012015>

Vanhala and Soininen 1995 . Laboratory technique for measurement of spectral induced polarization response of soil samples. *Geophysical Prospecting*, 43, 655–676.

Appendix A

Instrumentation



Figure A.1 Portable SIP field/lab Unit

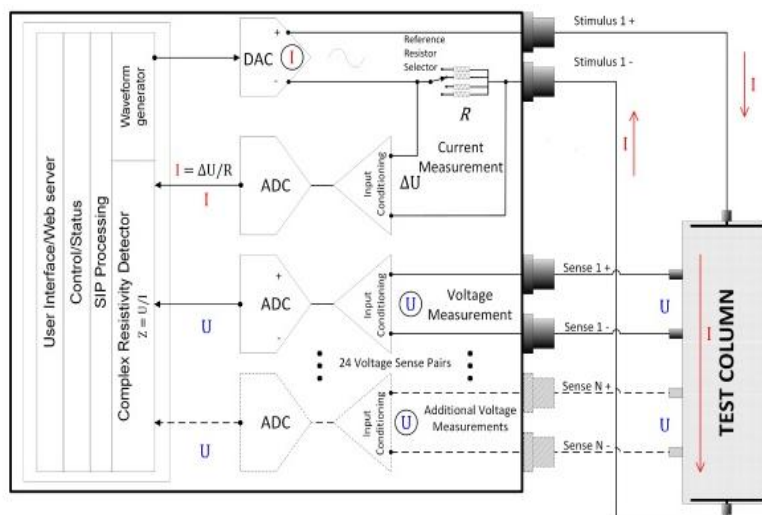


Figure A.2 Instruments inner diagram. (<http://www.ontash.com/products.htm>)(Kirmizakis 2016)

	<h2>Ontash & Ermac PSIP TOOL</h2>
<p>PSIP Unit Control</p> <p>Restart PSIP Software : <input type="button" value="Restart PSIP"/></p> <p>Reboot PSIP Unit : <input type="button" value="Reboot Server"/></p>	
<p>PSIP Firmware Update</p> <p>Click here to upload file</p> <p>Install Update : <input type="button" value="Install"/></p>	
<p>PSIP Measurements</p> <p>Stimulus Port-1 : <input type="button" value="Measurement-1"/></p> <p>Stimulus Port-2 : <input type="button" value="Measurement-2"/></p> <p>Stimulus Port-3 : <input type="button" value="Measurement-3"/></p> <p>Stimulus Port-4 : <input type="button" value="Measurement-4"/></p>	
<p>PSIP Processing</p> <p>Time Calculator : <input type="button" value="Calc"/></p>	
<p>Logging</p> <p>Click here to view logs folder</p>	

©2014 Ontash & Ermac, Inc.

Figure A.3 starting menu of the instrument. This is the page that you define the measurements parameters.

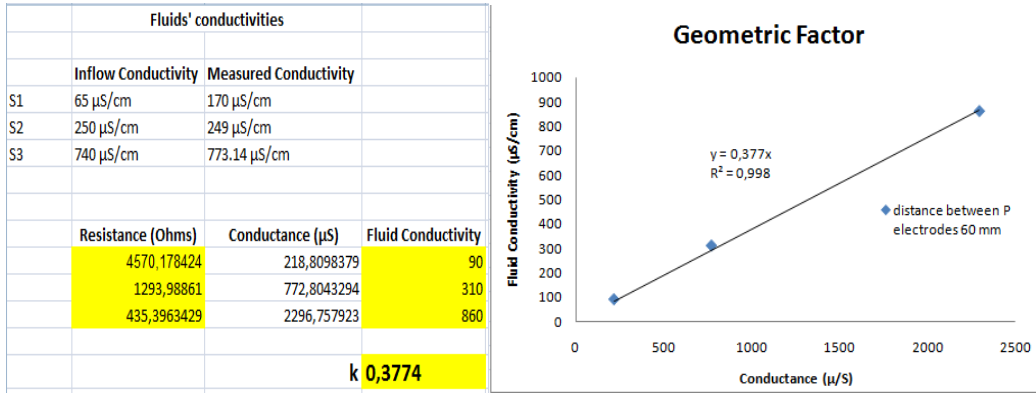


Figure A.5 Calculation of geometric factor for column 7 and electrode distance 0.6m.

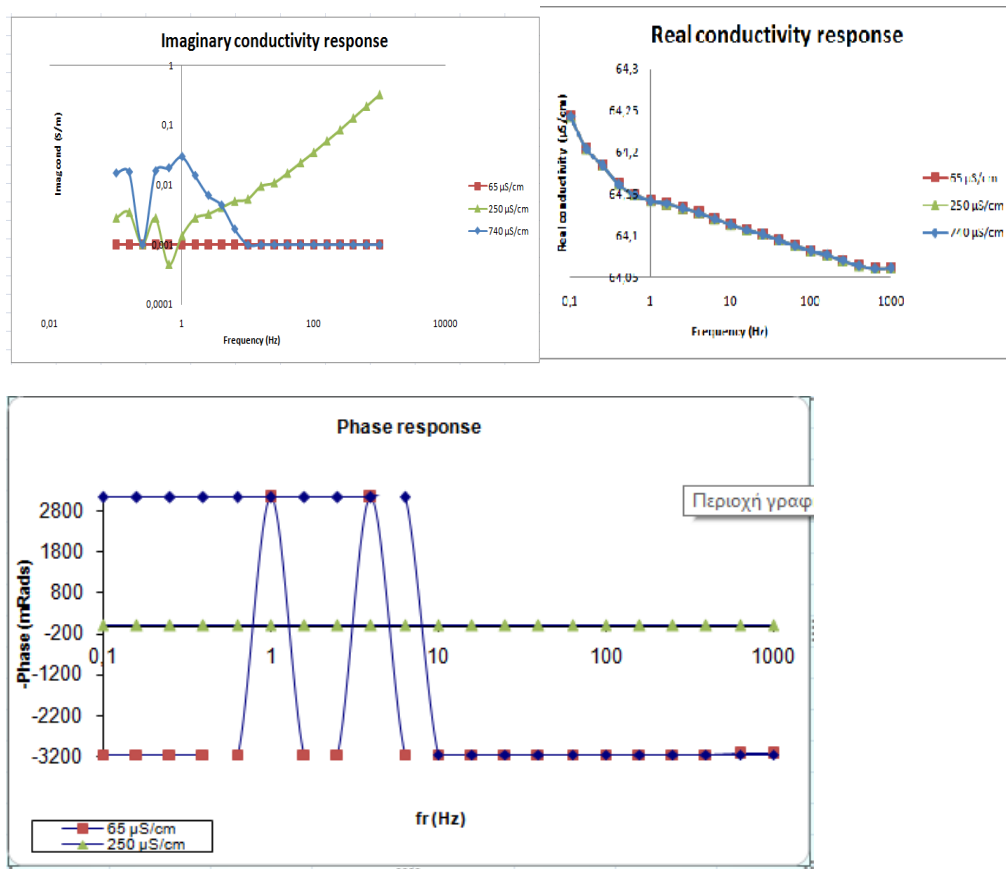


Figure A.6 Graphs from calibration measurements with the standard solution.

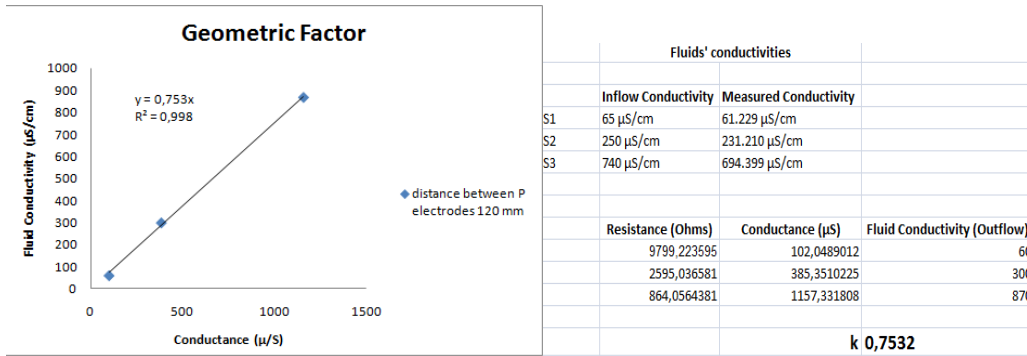


Figure A.7 Calculation of the geometric factor for column 1 and electrode combination (P1-P5).

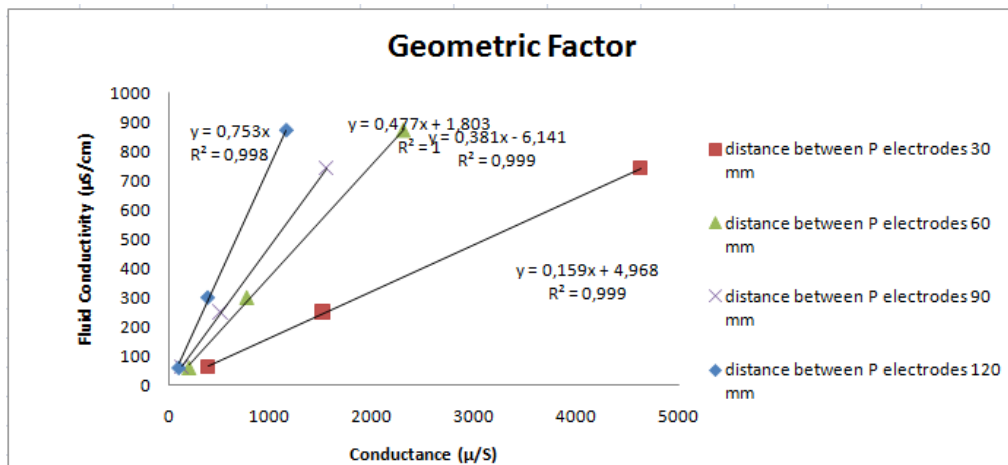
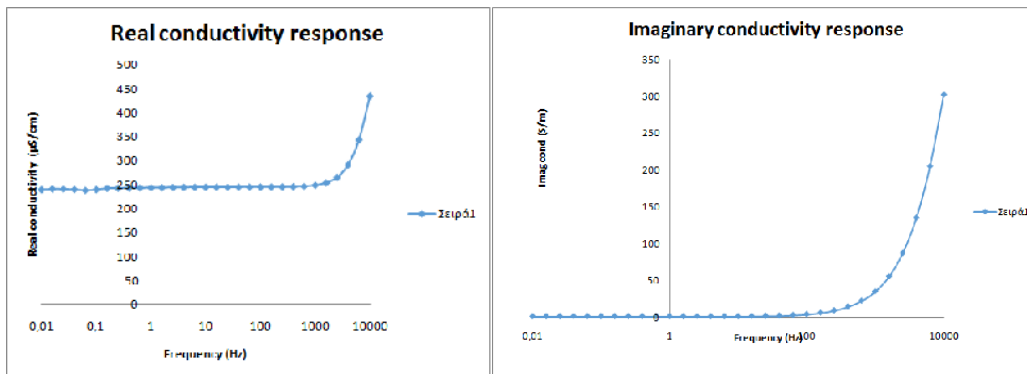


Figure A.8 Geometric factors diagram for column 1 and for four different electrode combinations.

Diagrams from the measurements with the TWW are presented; from each loop we export three graphs real and imaginary conductivity and the phase component for two electrode combinations (P1-P5) and (P2-P4).



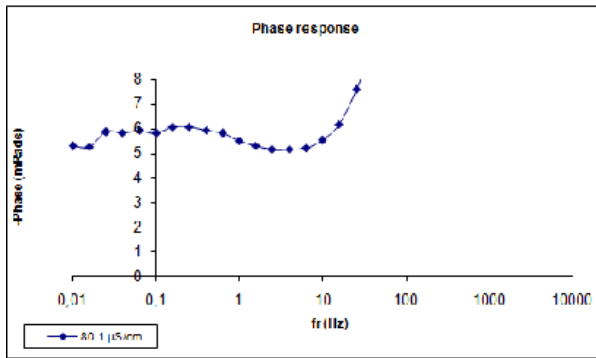


Figure A.9 Phase, imaginary and real conductivity diagrams for column 1(reference) for electrode combination (P1-P5).

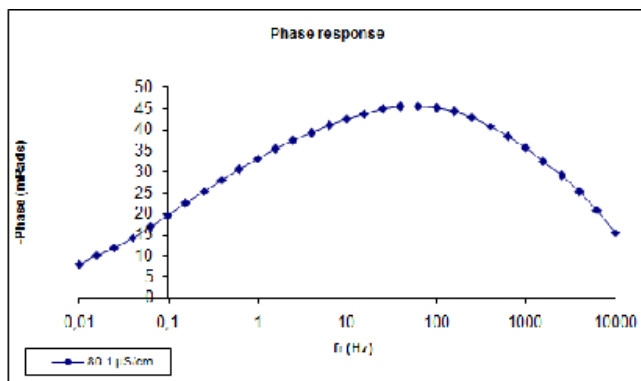
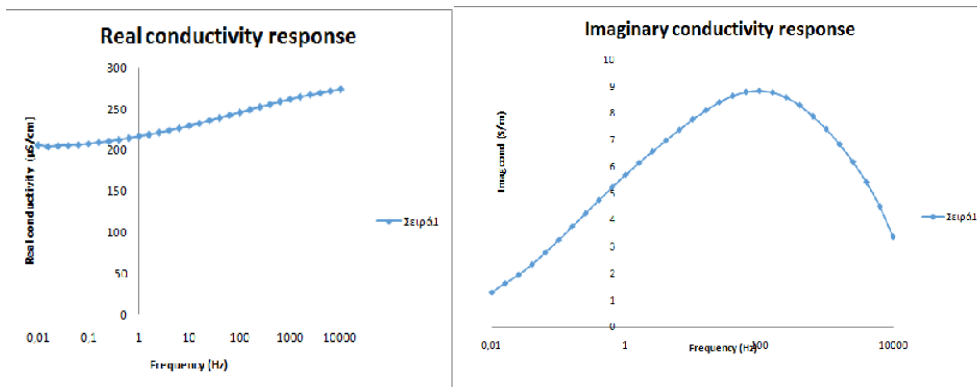


Figure A.10 Phase, imaginary and real conductivity diagrams for column 5(10% biochar) for electrode combination (P2-P4).

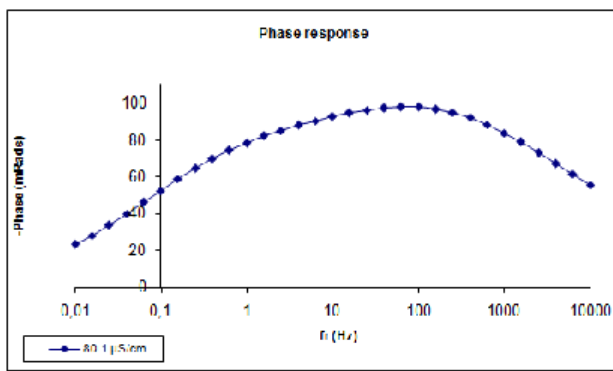
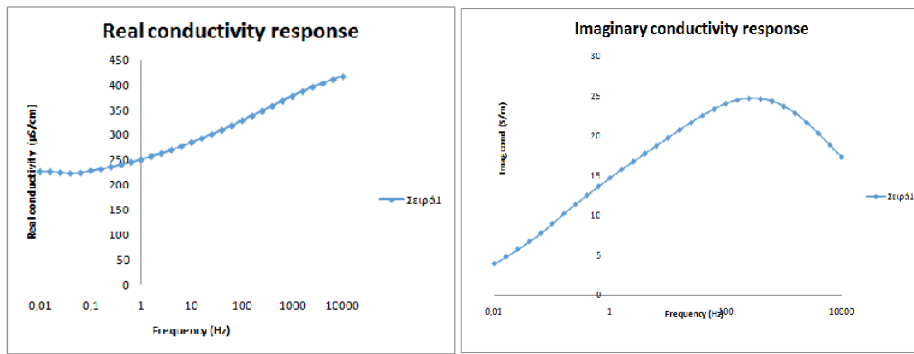
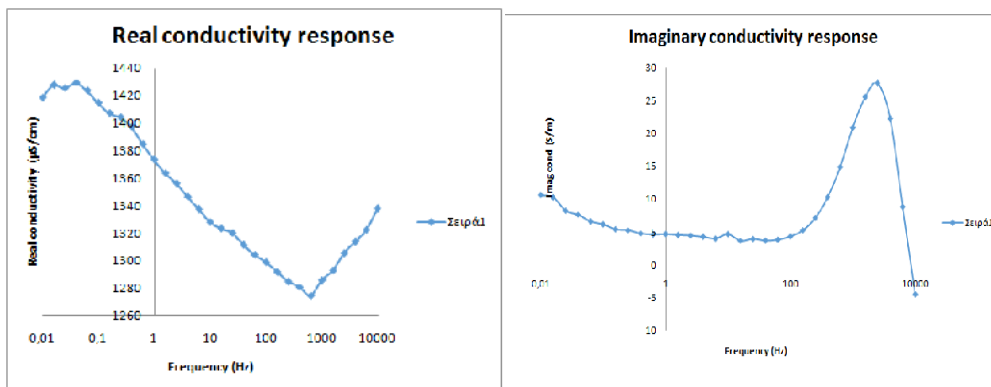


Figure A.11 Phase, imaginary and real conductivity diagrams for column 6(20% biochar) for electrode combination (P2-P4).



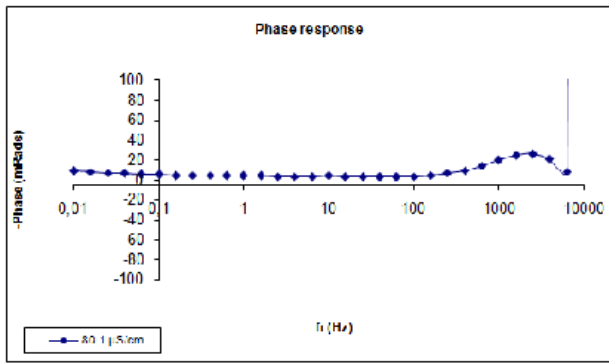


Figure A.12 Phase, imaginary and real conductivity diagrams for column 7(20% biochar) for electrode combination (P1-P5).

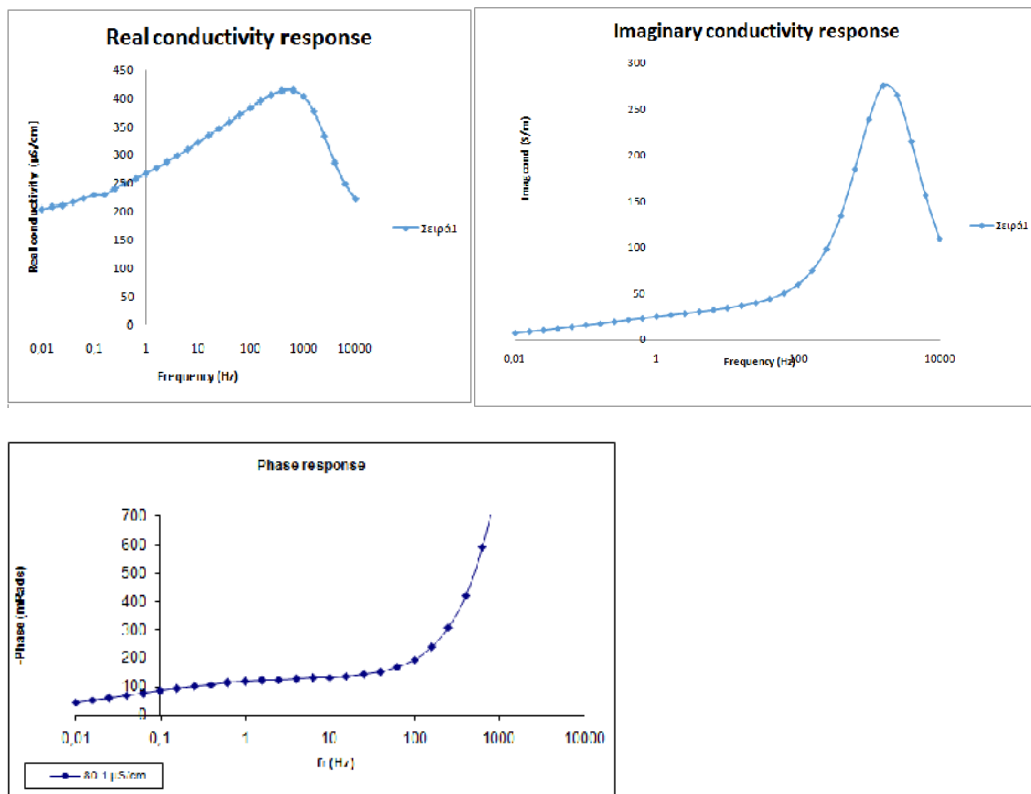


Figure A.13 Phase, imaginary and real conductivity diagrams for column 7(20% biochar) for electrode combination (P2-P4).

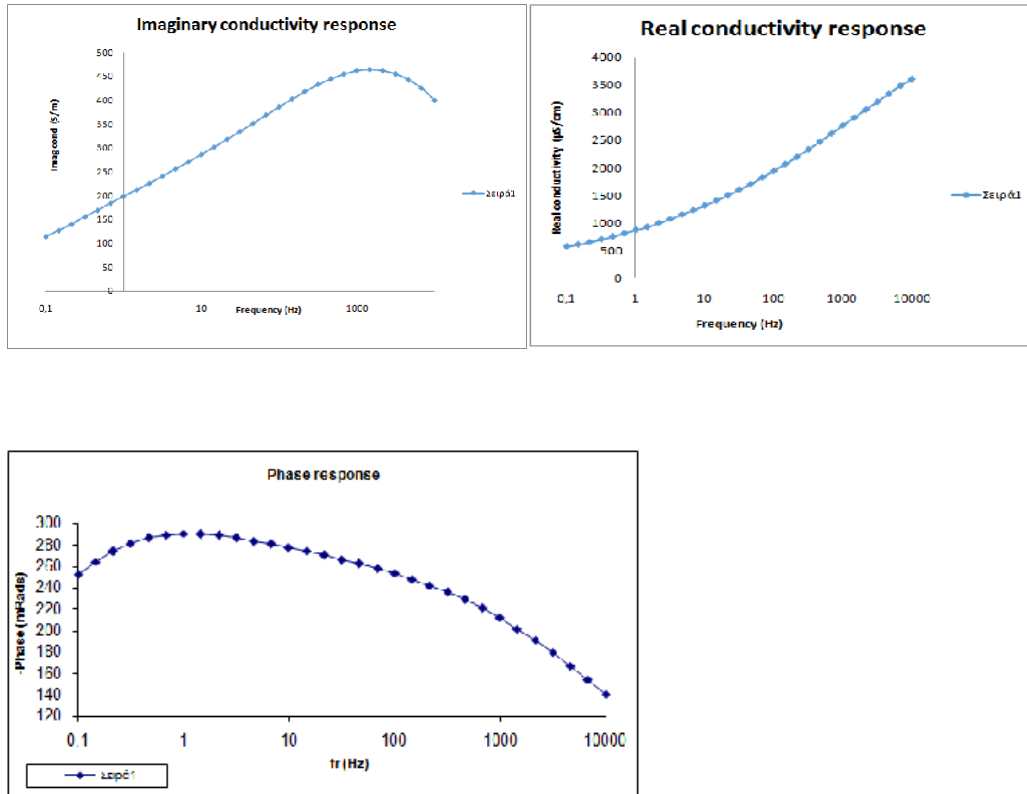


Figure A.14 Phase, imaginary and real conductivity diagrams for column 2(100% biochar) for electrode combination (P1-P5).

Conductivity tables are presented for the EC in situ measurements for each column.

Table A.1 Conductivity measurements for Column 6(20%) and RR120

C6:Step 20% biochar				
time(min)	collected fluid(ml)	sample	ml(sample	conductivity(μS/cm
36		1	15	1700
75		3	15	1500
112		5	15	1200
148		7	15	1300
183		9	15	1100
220		11	15	1000
256		13	16	1100
295		14	16	1100
329		16	15	1200
365		18	15	1000
406		19	18	1100
457		22	16	1200
494		23	13	1000
536		25	15	1000

Table A.2 Conductivity measurements for Column 7(20%) and RR120 in dynamic mode

C7:dynamic 20% biochar				
time(min)	collected fluid(ml)	sample	ml(sample	conductivity(μ S/cm)
55	80	2	15	1700
95	110	4	15	1300
127	190	6	15	1100
167	220	8	15	1000
210	280	10	15	990
259	300	12	15	1000
315	350	15	14	1000
354	390	17	16	1100
420	470	20	15	1000
460	510	21	17	1100
499	600	24	15	990
544	700	26	15	1100

Table A.3 Conductivity measurements for Column 2, dionised water and RR120

C2:100% biochar+dionised water				
time(min)	collected fluid(ml)	sample	ml/sample	conductivity(μ S/cm)
0		1	15	2720
20		2	15	1800
37		3	15	1670
42		4	15	1620
60		5	13	1560
77		6	13	1480
90		7	14	1360
105		8	15	1220

C2 :100% biochar+RR120				
time(min)	collected fluid(ml)	sample	ml/sample	conductivity(μ S/cm)
5	100	1	15	1100
12	150	2	15	1130
17	210	3	15	1130
24	230	4	11	1140
33	270	5	11	1170
42	280	6	11	1170
52	300	7	12	1200
61	310	8	11	1200
72	330	9	11	1210
84	340	10	12	1220
95	350	11	11	1220
100	360	12	15	1250
110	390	end		